Vibrational relaxation in simple fluids: Comparison of theory and simulation

M. Tuckerman[a] and B. J. Berne
Department of Chemistry and Center for Biomolecular Simulations, Columbia University, New York, New York 10027

(Received 17 November 1992; accepted 4 January 1993)

General theoretical expressions for the dephasing and energy relaxation times of a stiff oscillator in simple fluids are derived from the GLE and a critical discussion of the dynamic processes in these systems is given. In addition new methodological aspects of stochastic and full molecular dynamics simulations are discussed. The new reversible integrator based on the Trotter factorization of the classical propagator is used to directly simulate the vibrational energy and phase relaxation of a stiff classical oscillator dissolved in a Lennard-Jones bath. We compare the "real" relaxation from full MD simulations with that predicted by Kubo theory and by the generalized Langevin equation (GLE) with memory friction determined from the full molecular dynamics. It is found that the GLE gives very good agreement with MD for the vibrational energy relaxation, even for nonlinear oscillators far from equilibrium. The dephasing relaxation is also well approximated by the GLE.

I. VIBRATIONAL DEPHASING TIMES IN LIQUIDS

The modeling of vibrational energy transfer in fluids is an important problem in chemical physics that is germane to barrier crossing dynamics in the energy diffusion regime, dissociation kinetics, and vibrational relaxation. In a recent study indirect solvent coupling effects have been considered,[1] while other recent work has focused on non-Markovian effects where the vibrational displacement is described by the generalized Langevin equation (GLE),[2,3]

$$\mu\ddot{x}=-\frac{\partial W(x)}{\partial x}-\int_0^t d\tau\,\zeta(t-\tau)\dot{x}(\tau)+F(t), \qquad (1.1)$$

where x and $\dot{x}$ are, respectively, the position and velocity of the degree of freedom of interest, $W(x)$ is the potential of mean force on this coordinate, $F(t)$ is the random force, and $\zeta(t)$ is the memory friction. The second fluctuation–dissipation theorem[4] gives a relationship between the friction kernel and the autocorrelation function of the random force,

$$\zeta(t)=\beta\langle F(0)F(t)\rangle, \qquad (1.2)$$

where $\beta=(kT)^{-1}$. The GLE has played a very important role in the theory of liquids. Recently we have devised a method for extracting $\zeta(t)$ from molecular dynamics simulations and have used this method to determine the friction kernel on vibrational coordinates.[5–7] The explicit dynamic friction kernels so obtained can be used in stochastic simulations based on Eq. (1.1). In such simulations it is usually assumed that the random force is a Gaussian random process. Stochastic simulations consist of the following parts:

(a) Full molecular dynamics is used to find both the dynamic friction kernel and the potential of mean force on the reaction coordinate.

(b) The random force, assumed to be a Gaussian process, is sampled such that the second fluctuation–dissipation theorem is obeyed.

(c) The stochastic integrodifferential equation Eq. (1.1),[8,9] is numerically integrated.

We are now in a position to test the accuracy of the GLE on a model system consisting of one homonuclear diatomic molecule with a harmonic or anharmonic interatomic potential interacting with a Lennard-Jones (12–6) fluid through the same site–site Lennard-Jones (12–6) potential, i.e., the LJ parameters (ϵ,σ) are chosen to be the same for the solvent–solvent and for the molecule site–solvent atom interactions.

Theoretical treatments often show that the dephasing time T_2 and the energy relaxation time T_1 are related by

$$\frac{1}{T_2}=\frac{1}{2T_1}+\frac{1}{T_2^*}, \qquad (1.3)$$

where T_2^* is the pure dephasing time. If one can measure the pure dephasing time T_2^* and the energy relaxation time T_1, then the full dephasing time T_2 can be calculated from Eq. (1.3). Conversely, T_1 can be calculated given measurements of T_2 and T_2^*.

Molecular vibrations often have higher frequencies than the frequencies characterizing the solvent motion. Direct simulation of vibrational relaxation of systems with high and low frequency motion involves one of the most pervasive problems in the molecular dynamics literature, the problem of treating systems with a wide separation of time scales. A very small time step would be required for stable integration of the bonded vibrational motion and a very large number of integration time steps would be required to follow the nonbonded interactions. One way to

[a]In partial fulfillment of the Ph.D. in the Department of Physics, Columbia University.

 0021-9606/93/097301-18$06.00 © 1993 American Institute of Physics

bypass the direct simulation of the vibrational dynamics is to invoke the Kubo theory of dephasing.[10,11] Accordingly, the pure dephasing time T_2^* is given by

$$\frac{1}{T_2^*}=\int_0^\infty d\tau\langle\delta\omega(0)\delta\omega(t)\rangle, \tag{1.4}$$

where $\delta\omega(t)=\omega(t)-\bar{\omega}$ is the fluctuation of the vibrational frequency from the average vibrational frequency. It is important to recognize that the above theory is only approximate. In addition, this theory does not give T_1 nor does it give the contribution of energy relaxation to the dephasing time T_2^* [i.e., does not give a vibrational relaxation time in the form of Eq. (1.3)]. Simulations based on this approach are used to compute the autocorrelation function of the frequency. Oxtoby *et al.*[12,13] and Levine and Pollak[2] have shown using this approach that if $\delta\omega(t)$ is expanded in a power series involving spatial derivatives of the potential coupling the vibrational coordinate to the solvent it is an easy matter to determine the frequency fluctuation autocorrelation function from molecular dynamics. In this way they were able to study how molecular anharmonicity contributes to T_2^*.

Recently we have devised simple new integrators to treat systems with multiple time scales or disparate frequencies numerically.[14–16] Our new integrators allow us to use molecular dynamics to simulate vibrational phase and energy relaxation directly, even when the molecular vibrational frequency is very high compared to the frequencies in the spectral density of the solvent. Moreover, these same algorithms allow us to extract the dynamic friction on the harmonic bond. Thus it is now possible to determine the vibrational dephasing and energy relaxation of molecules in the liquid state without making any of approximations inherent in the Kubo theory.[10,11] Thus we can compare the relaxation dynamics from MD to what would be predicted from the simulation of the GLE with dynamic friction and potential of mean force determined from the MD simulation. This comparison is self consistent and any deviations from the predictions of the GLE will directly reflect on its accuracy and validity. This is especially important for anharmonic bonds for which case, the GLE can only be derived for very special cases. It is, therefore, important to study how well the GLE predicts the behavior of nonlinear systems. This can be done using an extension of the multiple time scale method for the GLE.

In this paper we study vibrational relaxation of the diatomic molecule as a function of vibrational frequency and anharmonicity. We use full multiple time scale molecular dynamics (NAPA or RESPA) to determine the full vibrational dynamics including T_1 and T_2 and $\zeta(t)$. We then perform multiple time scale GLE simulations using $\zeta(t)$ to determine the same properties. This allows comparison of MD, GLE, and theoretical predictions.

In Sec. II A we present the GLE theory. This section contains the derivation of an analytical expression for the GLE theory of energy relaxation—a new result as far as we can tell. In Sec. II B we derive dephasing times from the GLE for harmonic and cubic anharmonic diatomics. We show that Eq. (1.3) can be derived from a perturbation solution of the GLE, and the resulting expression for $1/T_2^*$ agrees with that derived by Oxtoby from quantum mechanical perturbation theory[12,13] and by Pollak from the harmonic bath Hamiltonian.[2] In Sec. III, we review the reversible NAPA and RESPA methods for MD and GLE simulations. In Sec. IV we compare the GLE, MD, and analytical results for both equilibrium and nonequilibrium simulations of the harmonic and anharmonic oscillator. Results are summarized in Sec. V.

Our purposes are twofold. First, we wish to test how well the generalized Langevin equation (GLE) predicts the true dynamics. Second, we wish to understand the role of molecular anharmonicity in vibrational relaxation. As a byproduct we will also investigate the accuracy of the Kubo theory.

II. PREDICTIONS OF THE GENERALIZED LANGEVIN EQUATION

The purpose of this part of the paper is to examine the predictions of the GLE for energy and vibrational relaxation times.

A. Energy autocorrelation function from the GLE

The generalized Langevin equation (GLE) for the bond stretch coordinate of a harmonic oscillator of reduced mass μ and vibrational frequency ω is

$$\ddot{x}=-\omega^2 x-\int_0^t d\tau\,\gamma(\tau)\dot{x}(t-\tau)+R(t), \tag{2.1}$$

where the dynamic friction on the bond is $\mu\gamma(t)\equiv\zeta(t)$ is related to the random force $R(t)\equiv F(t)/\mu$ through Eq. (1.2), which for $\gamma(t)$ and $R(t)$ becomes

$$\frac{\beta\gamma(t)}{\mu}=\langle R(0)R(t)\rangle. \tag{2.2}$$

The time correlation matrix is

$$\mathbf{C}(t)=\begin{bmatrix} C_{xx}(t) & C_{xv}(t) \\ C_{vx}(t) & C_{vv}(t)\end{bmatrix}, \tag{2.3}$$

where $C_{ab}(t)=\langle a(0)b(t)\rangle/\langle a^2\rangle$ are time correlation functions and the dynamic variables a and b are either x or v. The correlation functions are connected by the relations.

$$\dot{C}_{xx}(t)=C_{xv}(t)=-\omega^2 C_{vx}(t). \tag{2.4}$$

The random force $R(t)$ is often assumed to be a Gaussian random variable, from which it follows from Eq. (2.10) that $x(t)$ and $v(t)$ are also Gaussian random variables. For Gaussian stochastic processes

$$\begin{aligned}\langle a(t_1)b(t_2)c(t_3)d(t_4)\rangle &= \langle a(t_1)b(t_2)\rangle\langle c(t_3)d(t_4)\rangle+\langle a(t_1)c(t_3)\rangle \\ &\quad\times\langle b(t_2)d(t_4)\rangle+\langle a(t_1)d(t_4)\rangle\langle b(t_2)c(t_3)\rangle,\end{aligned} \tag{2.5}$$

where again a, b, c, d can each be either x or v. Such factorizations spring from the property of Gaussians that all the higher moments are determined by the first and second moments. This factorization can be used to compute $\langle\epsilon(0)\epsilon(t)\rangle$, the autocorrelation function of the har-

monic energy $\epsilon=\mu v^2/2+\mu\omega^2x^2/2$. This correlation function is a linear combination of four time correlation functions of the form $\langle a^2(0)b^2(t)\rangle$ each of which can be simplified using Eq. (2.5). For example,

$$\langle x^2(0)v^2(t)\rangle=\langle x^2\rangle\langle v^2\rangle+2\langle x(0)v(t)\rangle$$
$$=\langle x^2\rangle\langle v^2\rangle+2\frac{d}{dt}\langle x(0)x(t)\rangle. \tag{2.6}$$

Substituting these into $\langle\epsilon(0)\epsilon(t)\rangle$ together with the equilibrium moments, $\langle v^4\rangle=3(kT/\mu)^2$, $\langle x^4\rangle=3(kT/\mu\omega^2)^2$, and $\langle x^2v^2\rangle=(kT/\mu\omega)^2$ and the second fluctuation dissipation theorem, Eq. (2.2), allows us to recover a very simple expression for the decay of the energy fluctuations, an expression that involves the correlation functions directly calculated in MD and GLE simulations

$$C_{\epsilon\epsilon}(t)=\frac{\langle\delta\epsilon(0)\delta\epsilon(t)\rangle}{\langle\delta\epsilon^2(0)\rangle}=\frac{1}{2}C_{vv}^2(t)+\frac{1}{2}C_{xx}^2(t)+\frac{1}{\omega^2}\dot{C}_{xx}^2(t), \tag{2.7}$$

where $\delta\epsilon(t)\equiv\epsilon(t)-kT$.

Equation (2.7) can also be derived for the case when $R(t)$ is not a Gaussian random process as we now show. It is a simple matter to determine equations for the time correlation functions by sequentially multiplying the GLE by either $x(0)$ or $v(0)$ and averaging over a canonical distribution function. For example, the Laplace transform of the correlation function matrix is then

$$\tilde{\mathbf{C}}(s)=\frac{1}{\Delta(s)}\begin{pmatrix}s+\tilde{\gamma}(s) & -\tilde{\omega}^2\\ 1 & s\end{pmatrix}, \tag{2.8}$$

where

$$\Delta(s)=s^2+s\tilde{\gamma}(s)+\tilde{\omega}^2 \tag{2.9}$$

and we have used $\langle v(0)R(t)\rangle$ and $\langle x(0)R(t)\rangle=0$. In addition, one can derive solutions of the GLE for $x(t)$ and $v(t)$, in terms of these correlation functions

$$x(t)=x(0)C_{xx}(t)+v(0)C_{vx}(t)+\int_0^t d\tau\, R(t-\tau)C_{vx}(\tau),$$
$$v(t)=v(0)C_{vv}(t)+x(0)C_{xv}(t)+\int_0^t d\tau\, R(t-\tau)C_{vv}(\tau). \tag{2.10}$$

Equation (2.7) can therefore be obtained by substituting the squares of Eq. (2.10) into the energy correlation function, $\langle\delta\epsilon(0)\delta\epsilon(t)\rangle$ together with the second fluctuation dissipation theorem and some very simply derived identities such as

$$\int_0^{\tau_2}d\tau_1\,\gamma(\tau_2-\tau_1)C_{vv}(\tau_1)=\dot{C}_{xx}(\tau_2)-\dot{C}_{vv}(\tau_2) \tag{2.11}$$

and

$$\int_0^{\tau_2}d\tau_1\,\gamma(\tau_2-\tau_1)C_{vx}(\tau_1)$$
$$=-\frac{1}{\omega^2}\int_0^{\tau_2}d\tau_1\,\gamma(\tau_2-\tau_1)C_{xv}(\tau_1)=C_{xx}(\tau_2)-C_{vv}(\tau_2) \tag{2.12}$$

and additionally that correlation functions like $\langle v^{3}(0)R(t)\rangle$ vanish. The details of this derivation are given in Appendix A.

By a similar analysis, it is straightforward to show that the decay of the energy $\langle\delta\epsilon(t)\rangle_0$ from some initial state to its equipartition value of kT is given by

$$\langle\delta\epsilon(t)\rangle_{\{x(0),\dot{x}(0)\}}=\delta\epsilon_K(0)C_{vv}^2(t)+\delta\epsilon_P(0)C_{xx}^2(t)$$
$$+\delta\epsilon(0)\frac{1}{\omega_0^2}\dot{C}_{xx}^2(t), \tag{2.13}$$

where $\delta\epsilon_K(0)=\frac{1}{2}[\mu v^2(0)-kT]$, $\delta\epsilon_P(0)=\frac{1}{2}[\mu\omega_0^2x^2(0)-kT]$, and $\delta\epsilon(0)=\delta\epsilon_K(0)+\delta\epsilon_P(0)$. Note that our treatment here is exact. If the initial states are sampled from a microcanonical distribution for the oscillator for given $\epsilon(0)$, then it is easy to show that $\langle\delta\epsilon(t)\rangle_{\epsilon(0)}=\delta\epsilon(0)C_{\epsilon\epsilon}(t)$. In the next section, we will see how the high-frequency limit leads directly to the relation expressed in Eq. (1.3).

Thus we see that the explicit form of the energy correlation function given by Eq. (2.7) can be derived from the GLE under two different sets of assumptions:

(a) Either $R(t)$ is a Gaussian stochastic process;
(b) or $\langle v^n(0)R(t)\rangle=0$;
(c) and $\langle R(t_1)v^2(0)R(t_2)\rangle=\langle v^2(0)\rangle\langle R(t_1)R(t_2)\rangle$.

Nevertheless, both derivations of the energy correlation function are based on a restrictive set of assumptions about the random force $R(t)$. As we shall see later the GLE predicts an energy decay which is slightly different from molecular dynamics. Any deviation must be due to the breakdown of either of these sets of assumptions.

B. Dephasing times from the GLE

In this section, we examine the predictions of dephasing times from the GLE. This is a nontrivial calculation, and as far as we know our derivation of this quantity directly from the GLE has never been reported before.

1. Harmonic molecule

First we consider the simple case of the purely harmonic potential of mean force. From Eq. (2.8) the expression for the Laplace transforms of the velocity autocorrelation function is, $\tilde{C}_{vv}(s)=s/\Delta(s)$ and the displacement autocorrelation function, $\tilde{C}_{xx}(s)=[s+\gamma(s)]/\Delta(s)$, where $\Delta(s)$ is given by Eq. (2.9). Laplace inversion of these correlation functions requires an explicit form for the friction kernel. However, if $\tilde{\omega}\gg\tilde{\gamma}(0)$ (that is, if the frequency of the oscillator in solution is much larger than the static damping coefficient) perturbation solution of the dispersion equation

$$\Delta(s)=s^2+\tilde{\omega}^2+s\tilde{\gamma}(s)=0 \tag{2.14}$$

to first order in $\tilde{\gamma}(\tilde{\omega})/\tilde{\omega}$ is possible, giving the roots

$$s_\pm=\pm i[\tilde{\omega}+\tfrac{1}{2}\gamma''(\tilde{\omega})]-\tfrac{1}{2}\gamma'(\tilde{\omega})\equiv\pm i\Omega-\tfrac{1}{2}\gamma'(\tilde{\omega}), \tag{2.15}$$

where $\gamma'(\tilde{\omega})$ and $\gamma''(\tilde{\omega})$ are the real and imaginary parts of the Fourier–Laplace transform of the damping function

$$\tilde{\gamma}(i\tilde{\omega})=\int_0^\infty dt\, e^{-i\tilde{\omega}t}\gamma(t)\equiv\gamma'(\tilde{\omega})-i\gamma''(\tilde{\omega}). \quad (2.16)$$

Using Eq. (2.15), Laplace inversion of $\tilde{C}_{vv}(s)$ and $\tilde{C}_{xx}(s)$ is easily accomplished giving

$$C_{vv}(t)=\exp[-\tfrac{1}{2}\gamma'(\tilde{\omega})t]\left[\cos(\Omega t)-\frac{\gamma'(\tilde{\omega})}{2\tilde{\omega}}\sin(\Omega t)\right] \quad (2.17)$$

and

$$C_{xx}(t)=\exp[-\tfrac{1}{2}\gamma'(\tilde{\omega})t]\left[\cos(\Omega t)+\frac{\gamma'(\tilde{\omega})}{2\tilde{\omega}}\sin(\Omega t)\right]. \quad (2.18)$$

From the foregoing it follows that these correlation functions decay with an exponential envelope. The vibrational dephasing time for a stiff harmonic oscillator embedded in a fluid is easily seen from Eqs. (2.17) and (2.18) to be related to the real part of the frequency dependent damping function evaluated at the solvent shifted vibrational frequency.

$$\frac{1}{T_2}=\frac{1}{2}\gamma'(\tilde{\omega}). \quad (2.19)$$

As expected, the smaller the spectral density of the fluid at the solvent shifted vibrational frequency, the smaller will be $1/T_2$.

Since the velocity and position autocorrelation functions have exponential decay envelopes in the high frequency limit, it is clear from Eq. (2.7) that the energy decay will be approximated by a pure exponential function. This can be seen by substitution of Eqs. (2.17) and (2.18) into Eq. (2.7). The exponential decay rate then defines the energy relaxation time T_1 to be

$$\frac{1}{T_1}=\gamma'(\tilde{\omega}) \quad (2.20)$$

This is equivalent [cf. Eqs. (1.3) and (1.4)] to the well known result for purely harmonic systems that the dephasing rate contribution from energy relaxation is

$$\frac{1}{T_2}=\frac{1}{2T_1} \quad (2.21)$$

a result that cannot be derived from Kubo theory.

Before proceeding, it is useful to derive an approximate formula for convolution integrals involving the friction kernel. Consider any function $F(t)$ whose Laplace transform takes the form

$$\tilde{F}(s)=\frac{\tilde{f}(s)}{\Delta(s)}. \quad (2.22)$$

Therefore,

$$F(t)=\oint_C \frac{ds}{2\pi i}\frac{\tilde{f}(s)}{\Delta(s)}e^{st}, \quad (2.23)$$

where C is the usual Bromwich contour used for Laplace inversion.[17] Using the two roots in Eq. (2.15), it is a simple matter to show, by inverse Laplace transformation, that

$$\dot{F}(t)+\frac{\gamma'(\tilde{\omega})}{2}F(t)$$
$$=e^{-\gamma'(\tilde{\omega})t/2}[f'(\tilde{\omega})\cos(\Omega t)+f''(\tilde{\omega})\sin(\Omega t)] \quad (2.24)$$

and hence, that the convolution integral of $F(t)$ with $\gamma(t)$ is given approximately by

$$\int_0^t d\tau\,\gamma(\tau)F(t-\tau)=\oint_C\frac{ds}{2\pi i}e^{st}\tilde{\gamma}(s)\tilde{F}(s)$$
$$\approx\gamma'(\tilde{\omega})\left[1-\frac{\gamma''(\tilde{\omega})}{2\tilde{\omega}}\right]f(t)$$
$$-\frac{\gamma''(\tilde{\omega})}{\tilde{\omega}}\frac{df}{dt}. \quad (2.25)$$

This relation will be accurate in the stiff oscillator limit for which the roots in Eq. (2.15) are a good approximation. This formula will be very useful when analyzing the GLE for an anharmonic molecule, which we consider next.

2. Anharmonic molecule

The results in Sec. II A apply only to the pure harmonic oscillator. There is no pure dephasing contribution because the vibrational frequency is constant. The situation changes dramatically when one treats an anharmonic oscillator. In this case the vibrational frequency is coupled to the bath fluctuations and the frequency shifts due to the bath motion leads to frequency shifts and to dephasing according to the Kubo theory [cf. Eq. (1.4)]. The Kubo theory, however, ignores the contribution of the energy relaxation to dephasing. When the anharmonicity is weak it follows that the vibrational relaxation rate will be a superposition of that due to energy relaxation and that due to real dephasing. Our aim is to show that this assertion about the full vibrational relaxation time follows directly from the GLE.

The case we will consider is a potential that contains a cubic anharmonicity[12,13]

$$U(x)=\tfrac{1}{2}\mu\omega^2x^2+\tfrac{1}{6}fx^3, \quad (2.26)$$

where f gives the strength of the cubic anharmonicity. Using Kubo theory,[10,11] Oxtoby,[12,13] and later Pollak[2] showed that if the spectral density of the fluid is very small at the vibrational frequency the dephasing time is dominated by the anharmonicity; furthermore, if the anharmonicity can be considered a small perturbation to the harmonic force, then it can be shown that

$$\frac{1}{T_2}=\frac{f^2}{4\mu^3\omega^6\beta}\tilde{\gamma}(s=0), \quad (2.27)$$

where $\tilde{\gamma}(s=0)$ is the static damping rate. This dephasing rate will dominate over Eq. (2.19) only if $(f^2/4\mu^3\omega^6\beta)\times\tilde{\gamma}(s=0)\gg\gamma'(\tilde{\omega})/2$. Then the dephasing rate depends on the static friction instead of the frequency component of the friction. This raises an important issue when trying to simulate such systems. Harris has recently implemented a very rapid scheme for simulating the GLE. This scheme is based on a autoregression analysis which approximates the

true dynamic friction coefficient. Since the static friction requires knowledge of the full time dependence of the friction $[\tilde{\gamma}(s)=\int_0^\infty \gamma(t)dt]$, any error in the long time dependence can lead to serious errors in predicting the dephasing time. Unfortunately, this autoregression technique slows down considerably for such cases where accuracy is demanded for the static friction and becomes comparable to the methods used in this paper.

We now show how to derive the dephasing time of an anharmonic oscillator as given by Eq. (1.3) directly from the GLE. Consider a particle moving on a cubic potential of mean force surface $[W(x)=\mu\tilde{\omega}^2x^2/2+\tilde{f}x^3/6]$ for which the GLE reads

$$\ddot{x}=-\tilde{\omega}^2x-\frac{\tilde{f}}{2\mu}x^2-\int_0^t d\tau\,\dot{x}(\tau)\gamma(t-\tau)+R(t), \tag{2.28}$$

where $\tilde{\omega}$ and $\tilde{f}$ are the solvent shifted values of ω and f in Eq. (2.26). Note that the solvent shifted cubic coupling $\tilde{f}$ cannot be obtained from the harmonic bath Hamiltonian, but derives from the true expression for the potential of mean force

$$W(x)=-kT\ln g(x), \tag{2.29}$$

where $g(x)$ is the pair distribution function in x. Let us write the GLE in the following form:

$$\ddot{x}=-\frac{\partial W(x,t)}{\partial x}-\int_0^t d\tau\,\dot{x}(\tau)\gamma(t-\tau), \tag{2.30}$$

where

$$W(x,t)=W(x)-\mu R(t)x. \tag{2.31}$$

By completing the square, and changing variables to $y=x-R(t)/\omega$, the potential becomes

$$W(y,t)=\frac{1}{2}\mu\tilde{\omega}^2(t)y^2+\frac{1}{6}\tilde{f}\left[y+\frac{R(t)}{\tilde{\omega}}\right]^3, \tag{2.32}$$

where $\omega(t)\approx\tilde{\omega}+\tilde{f}R(t)/2\mu\tilde{\omega}^3\equiv\tilde{\omega}+\delta\omega(t)$. If we use this effective potential to establish a perturbation scheme for the GLE, then the lowest order expression is a linear equation which (expressed once more in terms of x) becomes

$$\ddot{x}=-\omega^2(t)x-\int_0^t d\tau\,\dot{x}(\tau)\gamma(t-\tau)+R(t). \tag{2.33}$$

Since we are interested in the high frequency limit as in the harmonic case, we may use Eq. (2.25) to approximate the convolution integral which appears in Eq. (2.33). The use of this relation assumes that the velocity $\dot{x}$ in the convolution integral assumes the form of Eq. (2.22) which, of course, is only true within the framework of perturbation theory. When this is done, Eq. (2.33) becomes

$$\ddot{x}\left[1-\frac{\gamma''(\tilde{\omega})}{\tilde{\omega}}\right]=-\omega^2(t)x-\gamma'(\tilde{\omega})\left[1-\frac{\gamma''(\tilde{\omega})}{2\tilde{\omega}}\right]\dot{x}+R(t). \tag{2.34}$$

Dividing by the coefficient of $\ddot{x}$, and dropping terms which go like $\gamma^2/\tilde{\omega}$ and higher, gives an approximate ordinary differential equation

$$\ddot{x}=-\Omega^2(t)x-\gamma'(\tilde{\omega})\dot{x}+R(t), \tag{2.35}$$

where $\Omega(t)=\tilde{\omega}+\gamma''(\tilde{\omega})/2+\tilde{f}R(t)/2\mu\tilde{\omega}^3\equiv\Omega+\delta\omega(t)$. Since we will be interested only in the position and velocity autocorrelation functions, on which the inhomogeneous term $R(t)$ has no effect, we need only consider solutions of the simpler homogeneous equation

$$\ddot{x}=-\Omega^2(t)x-\gamma'(\tilde{\omega})\dot{x}. \tag{2.36}$$

Note that $\delta\dot{\omega}/\delta\omega\sim 1/\tau_c$, where τ_c is the correlation time for the fluid and characterizes the decay of the friction kernel. Since the time scale for fluid motion is slow compared to the internal vibrations of the diatomic, it follows that $\delta\dot{\omega}/\delta\omega\ll\Omega$. Therefore, in constructing the solutions to Eq. (2.36), to a good approximation, we may take a linear combination of

$$\begin{aligned} x^{(+)}(t)&=x_0^{(+)}(t)e^{i\int_0^t\delta\omega(t')dt'},\\ x^{(-)}(t)&=x_0^{(-)}(t)e^{-i\int_0^t\delta\omega(t')dt'}, \end{aligned} \tag{2.37}$$

where $x_0^{(\pm)}(t)$ is a solution to Eq. (2.36) for $\delta\omega=0$ corresponding to $\exp(\pm i\Omega t)$ oscillatory dependence. By direct substitution into Eq. (2.36), it is straightforward to show that the two solutions in Eq. (2.37) satisfy the differential equation to order $\delta\dot{\omega}/\Omega\delta\omega$, a negligible contribution in the high frequency limit.

The position autocorrelation function $C_{xx}(t)$ is easily computed from the solutions (2.37) by multiplying by $x(0)$ and averaging. Consider the contribution to $C_{xx}(t)$ coming from $x^{(+)}(t)$

$$C_{xx}^{(+)}(t)=\langle x(0)x_0^{(+)}(t)e^{i\int_0^t\delta\omega(t')dt'}\rangle. \tag{2.38}$$

The average in the above expression can be separated into the product of two averages, one over the phase space of the oscillator, and the other over all possible realizations of $\delta\omega(t)$. The separation is possible because $x_0^{(+)}(t)$ does not depend on $\delta\omega(t)$. Thus, Eq. (2.38) becomes

$$C_{xx}^{(+)}(t)=C_{xx}^{(0+)}(t)\langle e^{i\int_0^t\delta\omega(t')dt'}\rangle, \tag{2.39}$$

where $C_{xx}^{(0+)}(t)$ is the contribution to the position correlation function for the harmonic oscillator with $\delta\omega=0$ coming from $x_0^{(+)}(t)$ as in Eq. (2.18). Assuming that $R(t)$ [hence $\delta\omega(t)$] is a Gaussian random variable makes it possible to use the cumulant theorem

$$\langle e^{i\int_0^t\delta\omega(t')dt'}\rangle=e^{-\int_0^t d\tau(t-\tau)\langle\delta\omega(0)\delta\omega(\tau)\rangle}. \tag{2.40}$$

The correlation function which appears in the exponent is just

$$\langle\delta\omega(0)\delta\omega(\tau)\rangle=\frac{\tilde{f}^2}{4\mu^2\tilde{\omega}^6}\langle R(0)R(\tau)\rangle=\frac{\tilde{f}^2}{4\mu^3\tilde{\omega}^6\beta}\gamma(\tau), \tag{2.41}$$

where we have used Eq. (2.2). Substituting back into the expression for the position autocorrelation function gives

$$C_{xx}^{(+)}(t)=C_{xx}^{(0+)}(t)\exp\left[-\left(\frac{\tilde{f}^2}{4\mu^3\tilde{\omega}^6\beta}\right)\int_0^t d\tau(t-\tau)\gamma(\tau)\right]. \tag{2.42}$$

Finally, extracting the long time decay of Eq. (2.42), and using the fact that $C_{xx}^{(0)}(t)$ decays exponentially as $\exp[-\gamma'(\tilde{\omega})t/2]$, we arrive at the expression for the decay time

$$\frac{1}{T_2}=\frac{\gamma'(\tilde{\omega})}{2}+\frac{\tilde{f}^2}{4\mu^3\tilde{\omega}^6\beta}\tilde{\gamma}(0). \tag{2.43}$$

We have used the fact that $\tilde{\gamma}(0)=\int_0^\infty \gamma(t')dt'$. The same result would have been obtained if we had used $C_{xx}^{(-)}(t)$ instead, and therefore, Eq. (2.43) is the overall decay rate of the position autocorrelation function. A similar analysis can be used to show that the velocity autocorrelation function $C_{vv}(t)$ decays in the same way so that one may study either of these correlation functions. Given that Eq. (2.43) is derived from perturbation theory, it can be expected to fail if f is chosen too large.

It is no surprise that the result is consistent with Eq. (1.3). The pure harmonic oscillator gives rise to the energy part of the vibrational relaxation time, while the lowest order contribution from the cubic anharmonicity is the dephasing time derived from Kubo theory starting from the harmonic bath Hamiltonian and applying perturbation theory. The harmonic bath Hamiltonian which takes the form[18,19]

$$H=\frac{p^2}{2\mu}+U(x)+\sum_\alpha\left[\frac{p_\alpha^2}{2m_\alpha}+\frac{1}{2}m_\alpha\omega_\alpha^2\left(y_\alpha-\frac{g_\alpha}{m_\alpha\omega_\alpha^2}x\right)^2\right], \tag{2.44}$$

where $U(x)$ is given by Eq. (2.26), is completely equivalent to the GLE when the identification

$$\zeta(t)=\sum_\alpha\frac{g_\alpha^2}{m_\alpha\omega_\alpha^2}\cos\omega_\alpha t, \tag{2.45}$$

$$R(t)=\frac{1}{\mu}\sum_\alpha g_\alpha\left\{\left[x_\alpha(0)-\frac{g_\alpha}{m_\alpha\omega_\alpha^2}q(0)\right]\cos\omega_\alpha t+\frac{p_\alpha}{m_\alpha\omega_\alpha}\sin\omega_\alpha t\right\}$$

is made. Clearly the $\zeta(t)$ and $R(t)$ in Eq. (2.45) manifestly satisfy the second fluctuation dissipation theorem Eq. (1.2). The equivalence of the harmonic bath Hamiltonian to the GLE means that one could just as well have started with this Hamiltonian and arrived at the expression Eq. (2.43) following the same perturbation scheme described above. It is worth noting, however, that the expression for the decay time does depend on the vanishing of $\langle v(0)R(t)\rangle$ as would be true for a Gaussian random process. The harmonic bath Hamiltonian Eq. (2.44) has been studied by Georgievskii and Stuchebrukhov[20] to determine line shape spectra for a cubic anharmonic diatomic. In their treatment, based on thermodynamic Green's functions, the coupling between the bath and the system coordinate x was treated to all orders, however, the cubic coupling was still treated as a small perturbation.

III. MOLECULAR AND STOCHASTIC DYNAMICS SIMULATIONS WITH MULTIPLE TIME SCALES

In order to test the limits of Kubo theory and perturbation theory of the GLE, it is necessary to consider extremely high frequency oscillators in relatively low frequency baths. In the systems considered here, a frequency ratio between oscillator and bath as high as 15 was considered. Even for moderate frequencies, there can be a substantial separation of time scales between the oscillator and the surrounding solvent atoms. Recently, we have developed algorithms (NAPA and RESPA), based on the choice of a reference system, to handle the separation of time scales in both the molecular dynamics and the stochastic dynamics simulations. In the case of the molecular dynamics, the reversible version of these algorithms as described in Ref. 21 have improved their performance considerably, and even though the GLE simulations are not reversible, the use of reversible RESPA methods have improved the performance in the GLE as well. We review the methods below.

The reversible NAPA and RESPA methods are based on the Trotter expansion of the classical Liouville propagator, $\exp(iL\Delta t)$, for a single time step Δt where the Liouville operator is $iL=\{\cdots,H\}$. H is the system Hamiltonian. Let x represent the relative coordinate of the oscillator, and let y represent all the solvent degrees of freedom and the center of mass motion of the diatomic. Then the Liouville operator for this system can be written in the form

$$iL=\frac{p_x}{\mu}\frac{\partial}{\partial x}+F_r(x)\frac{\partial}{\partial p_x}+f(x,y)\frac{\partial}{\partial p_x}+\frac{p_y}{m_y}\frac{\partial}{\partial y}+F_y(x,y)\frac{\partial}{\partial p_y}, \tag{3.1}$$

where $f(x,y)$ is the force on x due to the solvent. We choose a reference system for which the Liouville operator is $iL_r=(p_x/\mu)\partial/\partial x+F_r(x)\partial/\partial p_x$. Then $iL=iL_r+iL_y$, where iL_y contains all other terms in Eq. (3.1). The classical propagator is factorized according to the Trotter expansion

$$e^{iL\Delta t}=e^{iL_y\Delta t/2}e^{iL_r\Delta t}e^{iL_y\Delta t/2}+\mathcal{O}(\Delta t^3). \tag{3.2}$$

The derivatives in Eqs. (3.1) and (3.2) act on the initial conditions. The operator $e^{iL_y\Delta t/2}$ is further factorized such that the operator on the left of the reference system is written as

$$\exp\left(iL_y\frac{\Delta t}{2}\right)\approx\exp\left[\frac{\Delta t}{2}F_y(x,y)\frac{\partial}{\partial p_y}\right]\times\exp\left[\frac{\Delta t}{2}f(x,y)\frac{\partial}{\partial p_y}\right]\exp\left(\frac{\Delta t}{2}\dot{y}\frac{\partial}{\partial p_y}\right), \tag{3.3}$$

and the transpose of this is used for the operator on the right of the reference system. The resulting propagator is still reversible. When Eq. (3.3) and its transpose are substituted into Eq. (3.2), and the resulting operator is applied to an initial state $\{x(0),\dot{x}(0),y(0),\dot{y}(0)\}$, the following integration scheme emerges:

$$
\begin{aligned}
x(\Delta t) &= x_r\left[\Delta t; x(0), \dot{x}(0) + \frac{\Delta t}{2\mu} f(0)\right], \\
\dot{x}(\Delta t) &= \dot{x}_r\left[\Delta t; x(0), \dot{x}(0) + \frac{\Delta t}{2\mu} f(0)\right] + \frac{\Delta t}{2\mu} f(\Delta t), \\
y(\Delta t) &= y(0) + \Delta t \dot{y}(0) + \frac{\Delta t^2}{2m_y} F_y(0), \\
\dot{y}(\Delta t) &= \dot{y}(0) + \frac{\Delta t}{2m_y}\left[F_y(0) + F_y(\Delta t)\right],
\end{aligned}
\tag{3.4}
$$

where x_r and $\dot{x}_r$ represent the evolution of the position and velocity under the action of $\exp(iL_r\Delta t)$. A detailed discussion of the Liouville operator formalism is given in Ref. 21. This scheme has the nice feature that the solvent is integrated with pure velocity Verlet. Note that the velocity initial condition to the reference system is $\dot{x}(0) + (\Delta t/2\mu) f(0)$ rather than $\dot{x}(0)$. When $F_r(x)$ is a Hooke's law force $F_r(x) = -\mu\omega^2 x$, the analytical solution (the NAPA method) is readily obtained

$$
\begin{aligned}
e^{iL_r\Delta t} x(0) &= x(0)\cos\omega\Delta t + \frac{\dot{x}(0)}{\omega}\sin\omega\Delta t, \\
e^{iL_r\Delta t}\dot{x}(0) &= \dot{x}(0)\cos\omega\Delta t - \omega x(0)\sin\omega\Delta t.
\end{aligned}
\tag{3.5}
$$

Note that $\cos(\omega\Delta t)$ and $\sin(\omega\Delta t)$ only need to be computed once at the beginning of the simulation.

In the case that the potential contains a harmonic as well as cubic term $F_r(x) = -\mu\omega^2 x - fx^2/2$, an analytical solution is also available in terms of Jacobi elliptic functions. The details of the analytical solution are given in Appendix B. Although an analytical integration of the reference system is fast, the use of special functions can be cumbersome, in which case, a numerical integration scheme may be used (the RESPA method). This is implemented by defining a small time step $\delta t = \Delta t/n$ and writing $\exp(iL_r\Delta t)$ as

$$
\exp(iL_r\Delta t) = \left\{\exp\left[\frac{\delta t}{2} F_r(x)\frac{\partial}{\partial p_x}\right]\exp\left(\delta t \frac{p_x}{m}\frac{\partial}{\partial x}\right) \times \exp\left[\frac{\delta t}{2} F_r(x)\frac{\partial}{\partial p_x}\right]^n\right\} \tag{3.6}
$$

which, as has been shown by Tuckerman *et al.*,[16] yields n steps of velocity Verlet. Although there is a little more overhead in the numerical reference system, it is still an extremely efficient method.

Another possibility for factorizing the propagator exists which is useful when the solvent–solvent and solvent–solute forces contain long and short range components. By writing

$$
\begin{aligned}
F_y(x,y) &= F_{ys}(x,y) + F_{yl}(x,y), \\
f(x,y) &= f_s(x,y) + f_l(x,y),
\end{aligned}
\tag{3.7}
$$

where the s and l subscripts refer to the short and long range components, respectively, the propagator can be factorized as

$$
\begin{aligned}
\exp(iL\Delta t) = \exp\left[\frac{\Delta t}{2} F_{yl}(x,y)\frac{\partial}{\partial p_y}\right]\exp\left[\frac{\Delta t}{2} f_l(x,y)\frac{\partial}{\partial p_x}\right] \\
\times \exp(iL_s\Delta t)\exp\left[\frac{\Delta t}{2} f_l(x,y)\frac{\partial}{\partial p_x}\right] \\
\times \exp\left[\frac{\Delta t}{2} F_{yl}(x,y)\frac{\partial}{\partial p_y}\right],
\end{aligned}
\tag{3.8}
$$

where iL_s contains all the short range forces as well as the oscillator reference system. The operator $e^{iL_s\Delta t}$ is further broken up according to

$$
\begin{aligned}
e^{iL_s\Delta t} &= [e^{iL_s\delta t'}]^{n'}, \\
\exp(iL_s\delta t') &= \exp\left[\frac{\delta t'}{2} F_{ys}(x,y)\frac{\partial}{\partial p_y}\right]\exp\left[\frac{\delta t'}{2} f_s(x,y)\frac{\partial}{\partial p_x}\right] \\
&\times \exp\left(\frac{\delta t'}{2}\frac{p_y}{m_y}\frac{\partial}{\partial y}\right)\exp(iL_r\delta t')\exp\left(\frac{\delta t'}{2}\frac{p_y}{m_y}\frac{\partial}{\partial y}\right) \\
&\times \exp\left[\frac{\delta t'}{2} f_s(x,y)\frac{\partial}{\partial p_x}\right]\exp\left[\frac{\delta t'}{2} F_{ys}(x,y)\frac{\partial}{\partial p_y}\right],
\end{aligned}
\tag{3.9}
$$

and finally, the operator $e^{iL_r\delta t'}$ is written as $[e^{iL_r\delta t}]^n$ where now, $\delta t' = \Delta t/n'$ and $\delta t = \delta t'/n$. Putting this back into Eq. (3.9), and substituting Eq. (3.9) into Eq. (3.8), and acting with the resulting operator on an initial state gives the double RESPA integration scheme

$$
\begin{aligned}
x(\Delta t) &= x_s[\Delta t; x_r(t), \dot{x}_r(t), y(0)], \\
\dot{x}(\Delta t) &= \dot{x}_s[\Delta t; x_r(t), \dot{x}_r(t), y(0)] + \frac{\Delta t}{2m} f_t(\Delta t), \\
y(\Delta t) &= y_s\left[\Delta t; y(0), \dot{y}(0) + \frac{\Delta t}{2m} F_{yl}(0), x_r(t)\right], \\
\dot{y}(\Delta t) &= \dot{y}_s\left[\Delta t; y(0), \dot{y}(0) + \frac{\Delta t}{2m} F_{yl}(0), x_r(t)\right] + \frac{\Delta t}{2m} F_{yl}(\Delta t),
\end{aligned}
\tag{3.10}
$$

where y_s and $\dot{y}_s$ refer to the position and velocity of the solvent due to the action of the short range force and are generated by carrying out n' steps of velocity verlet with the short range forces starting with the initial conditions $\{y(0), \dot{y}(0) + (\Delta t/2m)F_{yl}(0)\}$ and using the numerical or analytical solution for the diatomic reference system. Similarly, x_s and $\dot{x}_s$ are generated by carrying out n' steps of the RESPA scheme

$$
\begin{aligned}
x(\delta t') &= x_r\left[\delta t'; x(0), \dot{x}(0) + \frac{\delta t'}{2m} f_s(0)\right], \\
\dot{x}(\delta t') &= \dot{x}_r\left[\delta t'; x(0), \dot{x}(0) + \frac{\delta t'}{2m} f_s(0)\right] + \frac{\delta t'}{2m} f_s(\delta t'),
\end{aligned}
\tag{3.11}
$$

where x_r and $\dot{x}_r$ refer to the position and velocity of x due to the bond potential which can either be integrated analytically, or using n little time steps of size δt.

The application of NAPA and RESPA to the GLE has been discussed in Ref. 16. We now modify that discussion to include the reversible scheme discussed above. The GLE reads

$$\mu\ddot{x}=f(x)-\int_0^t d\tau\,\zeta(\tau)\dot{x}(t-\tau)+F(t), \tag{3.12}$$

where $f(x)=-\partial W/\partial x$. We take the reference force $F_r(x)=f(x)$, and the remaining part

$$\Delta F(\dot{x})=-\int_0^t d\tau\,\zeta(\tau)\dot{x}(t-\tau)+F(t) \tag{3.13}$$

which when written in discrete form becomes

$$\Delta F_n=-\Delta t\sum_{k=0}^{n} w_k\zeta_k\dot{x}_{n-k}+F_n \tag{3.14}$$

and

$$\Delta F_{n+1}=-\Delta t\sum_{k=0}^{n+1} w_k\zeta_k\dot{x}_{n+1-k}+F_{n+1}. \tag{3.15}$$

The w_k's are Newton–Cotes weights in the numerical integration method (e.g., $w_0=w_n=1/2, w_1=\cdots=w_{n-1}=1$ for the trapezoid rule). Velocity Verlet requires ΔF_{n+1} in order to determine $\dot{x}_{n+1}$ and ΔF_{n+1} involves $\dot{x}_{n+1}$. We therefore separate this term out of ΔF_{n+1} by writing

$$\Delta F_{n+1}=\Delta F'_{n+1}-\Delta t w_0\zeta_0\dot{x}_{n+1}. \tag{3.16}$$

The force is used to derive a RESPA scheme for the GLE based on the Trotter expansion. When, we solve for $\dot{x}_{n+1}$, the following algorithm emerges:

$$\begin{aligned} x_{n+1}&=x_r\left[\Delta t; x_n,\dot{x}_n+\frac{\Delta t}{2\mu}\Delta F_n\right], \\ \dot{x}_{n+1}&=\frac{\dot{x}_r[\Delta t; x_n,\dot{x}_n+(\Delta t/2\mu)\Delta F_n]+(\Delta t/2\mu)\Delta F'_{n+1}}{1+(\Delta t^2 w_0\zeta_0/2\mu)}, \end{aligned} \tag{3.17}$$

where, as usual x_r and $\dot{x}_r$ refer to the reference system position and velocity evolved using $\exp(iL_r\Delta t)$. The reference system can be evaluated analytically or numerically as before. In both the MD and GLE simulations, Δt may be chosen according to the time scale of the solvent motion without loss of accuracy.

IV. RESULTS

The system studied consisted of 64 Lennard-Jones particles at reduced temperature $\hat{T}=2.5$ and reduced density $\rho\sigma^3=1.05$ in which is imbedded a single diatomic with either a harmonic or cubic bond potential. Some of the cases considered here were run using 500 particles to check system size dependence, and these were found to agree with the small system results. The diatomic is kept at a fixed spatial orientation along a body diagonal of the cubic cell so that rotational anharmonicities are not present. Using the integrator of Eq. (3.4), simulations were run for 2×10^6 or more steps using a big time step of 2×10^{-3} in all cases. Each run required approximately 5.5 h of CPU time per 10^6 steps on an IBM 3090 vector processor. The energy conservation was measured by the following formula:

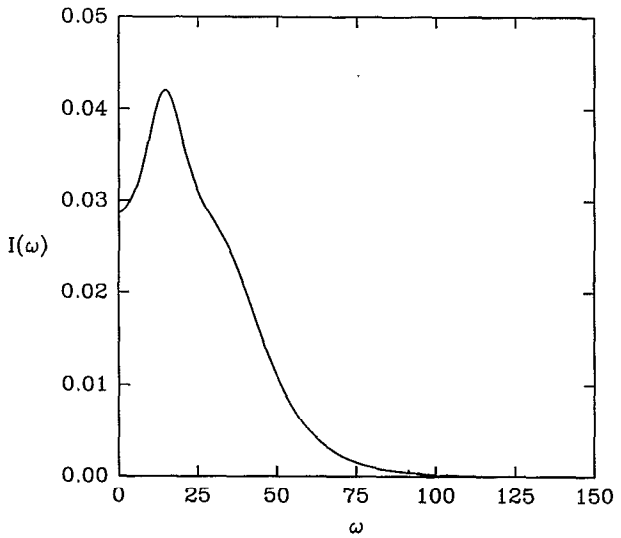

FIG. 1. The spectral density of a pure Lennard-Jones fluid at $\hat{T}=2.5$ and $\rho\sigma^3=1.05$ as computed from the Fourier transform of the single particle velocity autocorrelation function.

$$\Delta\hat{E}\equiv\frac{1}{N}\sum_{k=1}^{N}\left|\frac{E_k-E_0}{E_0}\right|, \tag{4.1}$$

where E_0 is the initial energy of the system. In all simulations, this time step gave energy conservation $\Delta\hat{E}\sim10^{-3}$ measured in this manner independent of frequency or cubic coupling.

A. Harmonic diatomic imbedded in Lennard-Jones fluid

The first set of studies were carried on a harmonic diatomic $U(x)=\mu\omega^2x^2/2$, with frequency choices of $\omega=60$, 90, 120, and 150. For the harmonic potential, we use an analytic reference system solution with the reversible NAPA scheme in Eq. (3.4). To see how the time scales of the oscillator compare with that of the surrounding fluid, we plot the spectral density of the neat fluid in Fig. 1. The peak of the spectral density is around $\omega=20$, and it can be seen that $\omega=60$ and 90 are well within the significant part of the spectral density, whereas 120 and 150 are not, so that there is a sharp separation of time scales between the solvent and the vibrational motion of the diatomic at the two higher frequencies. The manifestation of this time scale separation can be seen in Fig. 2 in which we plot the decay envelopes of the velocity autocorrelation functions of the oscillator at the four frequencies. There is a drastic increase in the decay time between $\omega=90$ and $\omega=120$. This is also manifest in the decay time of the energy autocorrelation functions plotted in Fig. 3. The energy of the bond is taken to be

$$\epsilon=\tfrac{1}{2}\mu\dot{x}^2+U(x) \tag{4.2}$$

which does not include the interaction with the surrounding solvent atoms.

To test the predictions based on the GLE, it is necessary to carry out simulations in which the GLE is inte-

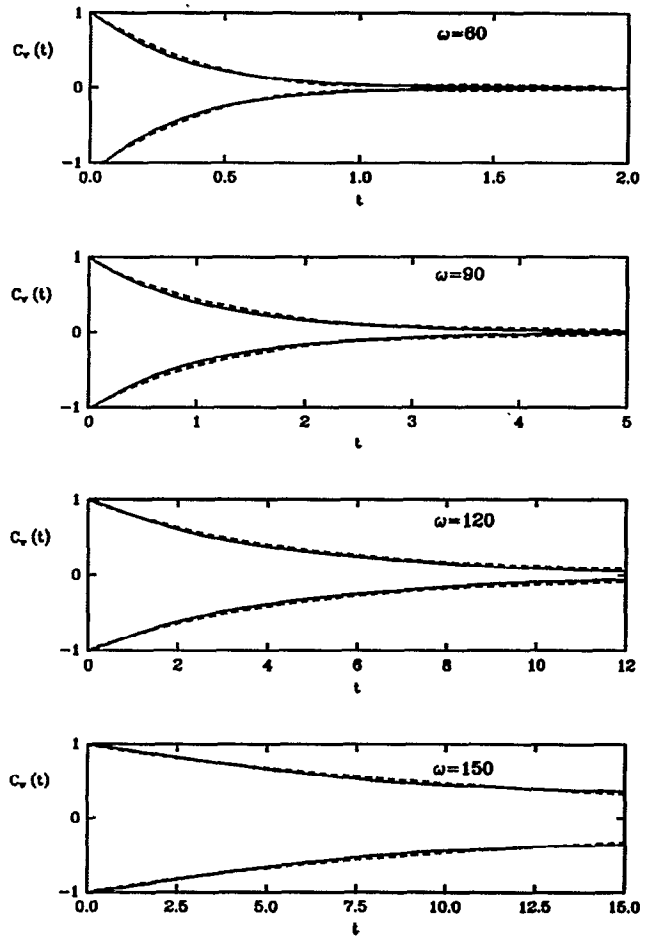

FIG. 2. Decay envelopes of the velocity autocorrelation functions from MD (solid line) and GLE (dashed line) simulations for a harmonic oscillator in Lennard-Jones fluid for $\omega=60$, 90, 120, and 150.

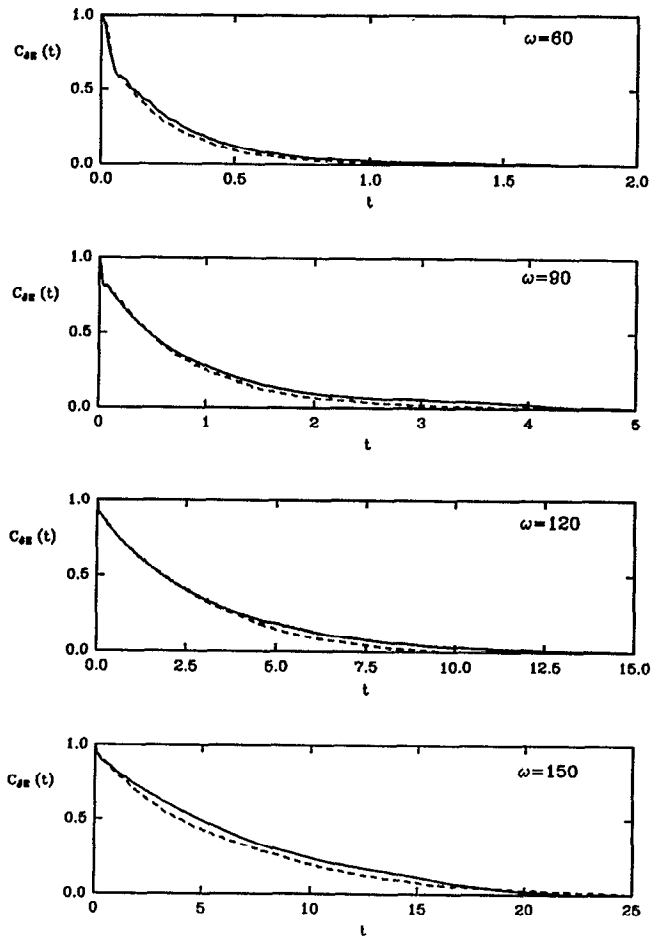

FIG. 3. Full energy autocorrelation functions from MD (solid line) and GLE (dashed line) simulations of a harmonic oscillator in Lennard-Jones fluid for $\omega=60$, 90, 120, and 150.

grated numerically. The inputs to the GLE are a friction kernel $\xi(t)$, and a random force $R(t)$ such that the second fluctuation dissipation theorem Eq. (2.2) is satisfied. One way to obtain the friction kernel from molecular dynamics is the method of Straub and Berne.[5] If we multiply the GLE for the harmonic oscillator on both sides by $\dot{x}$ and average over a canonical ensemble, we obtain a memory function equation of the Volterra type for the velocity autocorrelation function

$$\dot{C}_{vv}(t) = -\int_0^t d\tau\, K(t-\tau) C_{vv}(\tau), \tag{4.3}$$

where the kernel $K(t) \equiv \tilde{\omega}^2 + \gamma(t)$. Using the velocity autocorrelation function from the molecular dynamics simulations, it is a simple matter to invert the memory function equation to obtain the friction kernel. It should be noted, however, that the inversion process is stable only at low frequency, and in this case works well only for the cases $\omega=60$ and 90. Stability in this procedure can be improved if one calculates the correlation functions $C_{xx}(t)$, $C_{xv}(t)$, and $C_{vv}(t)$ directly from MD and uses these in Eq. (4.3). To find the friction for the case of an extremely high frequency diatomic, the friction on the bond may be approximated by the friction on a rigid bond.[7] It is shown in Ref. 7 that in the infinite frequency limit, the true friction and the friction on the rigid bond are equal. In Fig. 4(a), we show the friction kernels as a function of time for the case $\omega=60$ and for the rigid bond, and in Fig. 4(b), we show the corresponding Fourier transforms.

The random force can be obtained in a simple way if it is assumed that $R(t)$ is a Gaussian random process. Then the method of Rice can be used.[22–24] The random force is expanded in a Fourier series

$$R(t) = \sum_{k=1}^{P} [a_k \sin \omega_k t + b_k \cos \omega_k t], \tag{4.4}$$

where $\omega_k = 2\pi k/P\Delta t$ and P is the number of points in each trajectory. The Fourier coefficients a_k and b_k are sampled independently from a Gaussian distribution

$$P(a_k, b_k) = \frac{1}{\sqrt{4\pi\sigma_k^2}} e^{-(a_k^2+b_k^2)/2\sigma_k^2}, \tag{4.5}$$

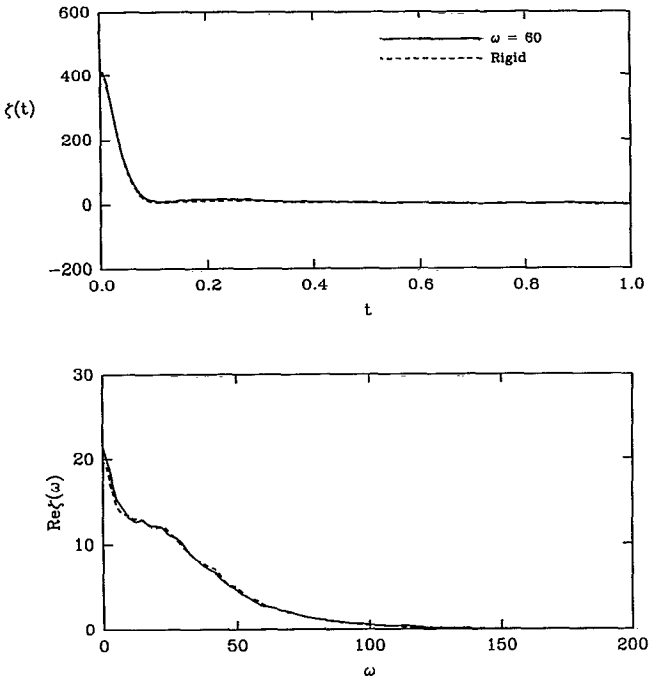

FIG. 4. The friction kernel used in the GLE simulations as computed using the method of Straub and Berne (Ref. 5) based on Eq. (4.3) (solid line) and using the method of Berne *et al.* from the velocity autocorrelation function on a rigid bond (dashed line). The upper curve shows the time dependent friction kernel, and the lower curve shows the frequency dependence from the Fourier cosine transform.

where σ_k^2 is related to the Fourier transform of the friction kernel

$$\sigma_k^2=\frac{1}{P}\sum_{j=0}^{P}\zeta(j\Delta t)e^{-2\pi ijk/P} \tag{4.6}$$

which is easily accomplished by fast Fourier transforms. To carry out the simulation, one samples an ensemble of initial conditions from a canonical distribution and evolves each according to the GLE using the friction and random force scheme above along with an integrator like that of Eq. (3.17). Observable quantities are calculated by averaging over each trajectory and over the ensemble of trajectories.

GLE simulations were carried out on the diatomic for the four frequencies discussed above using an analytic reference system. The GLE requires not the bare frequency ω but the renormalized frequency $\tilde{\omega}$ from the potential of mean force. The potential of mean force surface for this problem has been fit by Straub *et al.*,[25] and we use the renormalized frequencies from this fit which are for bare frequency values $\omega=60$, 90, 120, and 150, $\tilde{\omega}=59.447$, 89.632, 119.724, and 149.780, respectively. The decay envelopes of the velocity autocorrelation functions calculated from the GLE are plotted along with the MD results in Fig. 2. We see that the agreement between molecular dynamics and the GLE is very good in these cases, and hence the predictions of $1/T_2$ should be in good agreement. In Table I, we show the values of $1/T_2$ for each value of ω as

TABLE I. Vibrational relaxation rates for harmonic oscillator from MD, GLE, and Eq. (2.19).

ω	$\left(\frac{1}{T_2}\right)_{\mathrm{MD}}$	$\left(\frac{1}{T_2}\right)_{\mathrm{GLE}}$	$\frac{\gamma'(\tilde{\omega})}{2}$
60	2.71	2.70	2.97
90	0.74	0.73	0.78
120	0.19	0.18	0.18
150	0.08	0.08	0.08

predicted by MD, by the GLE, and by perturbation theory on the GLE [cf. Eq. (2.19)]. We see that as the frequency increases, the GLE simulation results and the GLE perturbation theory results come into closer agreement as expected, since the perturbation theory assumed high frequency. The MD and GLE agree well at all frequencies. In Fig. 3, we show the energy autocorrelation functions from the GLE together with the MD. The GLE energy autocorrelation functions can be computed directly from the simulation or using the formula Eq. (2.7). These results serve as a test of the assumption of a Gaussian random force. It is interesting to note that the GLE autocorrelation functions consistently decay faster than those from the MD although the discrepancy is small. In Table II, we show the values of $1/T_1$ for each value of ω for the MD, GLE, and GLE perturbation theory. Again, we see a consistently small discrepancy between the GLE and MD results. In Fig. 5, we show that the solvent force is not well described by Gaussian statistics by plotting the autocorrelation function of the square of the random force computed in the MD simulations using the formula

$$R(t)=\mu\ddot{x}+\mu\tilde{\omega}^2x^2+\int_0^t d\tau\,\zeta(t-\tau)\dot{x}(\tau). \tag{4.7}$$

If $R(t)$ is a Gaussian random process, then, since $\langle R(t)\rangle=0$, the autocorrelation function of the square of the random force should be given by

$$\langle R^2(0)R^2(t)\rangle=\langle R^2(0)\rangle^2+2\langle R(0)R(t)\rangle^2. \tag{4.8}$$

The solid line in Fig. 5 shows the autocorrelation function of the square of $R(t)$ and the dashed line shows the plot of the factorization based on Eq. (4.8). The top curve is for a diatomic with frequency $\omega=60$ and the bottom curve is for a frequency of $\omega=150$. We see that the higher the frequency, the more dramatic the departure of the random force statistics from that those of a Gaussian random pro-

TABLE II. Energy relaxation rates for harmonic oscillator from MD, GLE, and Eq. (2.20).

ω	$\left(\frac{1}{T_1}\right)_{\mathrm{MD}}$	$\left(\frac{1}{T_1}\right)_{\mathrm{GLE}}$	$\gamma'(\tilde{\omega})$
60	5.10	5.56	5.94
90	1.36	1.45	1.56
120	0.34	0.36	0.36
150	0.14	0.15	0.15

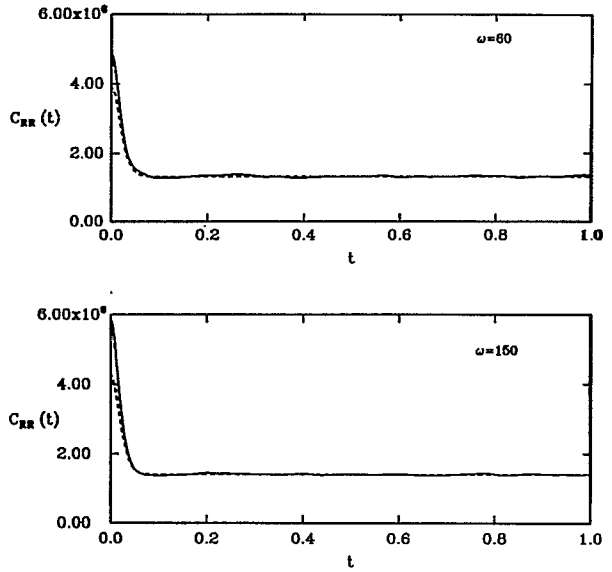

FIG. 5. The autocorrelation function of the square of the random force as computed from MD using Eq. (4.7) (solid line) and the Gaussian approximation to this correlation function from Eq. (4.8) (dashed line) for $\omega=60$ (upper curve) and $\omega=150$ (lower curve).

cess. It is also interesting to note that the initial value $\langle R^4(0)\rangle$ is consistently larger than the prediction $3\langle R^2(0)\rangle^2$ of Eq. (4.8). This fact suggests that for short times, the statistics of the solvent force (which will be determined by strong collisions coming from the short range part of the force) are non-Gaussian and we conjecture that these should be treated as a Poisson process.

A possible explanation for the small discrepancy between the GLE and molecular dynamics is the following. In the real fluid the vibrational displacement suffers infrequent strong collisions and frequent soft collisions. Strong collisions occur when energetic solvent atoms approach either of the atomic sites on the molecule very closely. These are binary collisions and should be described by statistics that are more like Poisson statistics. The soft collisions are due to the superposition of longer range forces from many solvent atoms and thus, according to the central limit theorem, should be described by the statistics of Gaussian random variables. We find, consistently, that Gaussian statistics gives rise to faster energy relaxation than what is observed from the MD simulations. It is a straightforward but tedious matter to expand the difference, $\Delta_\epsilon^{(4)}(t)$, between the normalized energy autocorrelation function and its Gaussian approximate Eq. (2.7) to order $\mathcal{O}(t^4)$ (see Appendix C for details),

$$\frac{\Delta_\epsilon^{(4)}(t)}{t^4}=\frac{1}{8\mu^2}\left\langle\left[\frac{\partial^2U}{\partial x^2}-\left\langle\frac{\partial^2U}{\partial x^2}\right\rangle\right]^2\right\rangle + \frac{\tilde{\omega}^2}{24\mu}\left\langle\frac{\partial^2U}{\partial x^2}\left[\beta\mu\tilde{\omega}^2x^2-1\right]\right\rangle + \frac{1}{24\beta\mu^2}\left\langle\frac{\partial^4U}{\partial x^4}\right\rangle-\frac{\tilde{\omega}^2}{12\mu}\left\langle\frac{\partial^3U}{\partial x^3}x\right\rangle, \quad (4.9)$$

but in the high-frequency limit, the deviation becomes

$$\Delta_\epsilon^{(4)}(t)\to\frac{(\tilde{\omega}t)^4}{24kT}\left\langle x^2\frac{\partial^2U}{\partial x^2}\right\rangle\geqslant 0. \quad (4.10)$$

This inequality holds unless soft modes and barrier crossing are dominant. Thus for a stiff oscillator, we expect, for short times at least, that the energy decay predicted by the GLE will be faster than for the real system.

It should be possible to develop a model which includes both Gaussian and Poissonian collisions in the GLE in such a way that Eq. (2.2) is satisfied. This would describe the situation envisioned here where the molecule suffers frequent soft collisions punctuated infrequently by strong collisions. This has the flavor of the old Rice–Allnatt theory of liquids,[26,27] and similar effects were discussed by Berne *et al.*[28] It should be noted that such models could be important when strong infrequent pair interactions contribute to the energy relaxation. We expect that the stiffer the oscillator, and the lower the solvent density, the more important such effects might be.

B. Anharmonic diatomic imbedded in Lennard-Jones fluid

The second set of studies were carried out on an anharmonic diatomic molecule with bond potential $U(x)=\mu\omega^2x^2/2+fx^3/6$ imbedded in the same Lennard-Jones fluid. Each simulation requires a value for ω and f. The parameters chosen were $f=10\,000$ for $\omega=60$, $f=30\,000$ for $\omega=90$, $f=90\,000$ for $\omega=120$, $f=1.8\times10^5$ for $\omega=150$, and $f=1.0\times10^6$ for $\omega=300$. It is worth examining in what sense these values for f are perturbations on the harmonic potential. The cubic potential has its maximum at $x_c=-2\mu\omega^2/f$, and the height of the maximum is

$$V_c=\frac{2\mu^3\omega^6}{3f^2}. \quad (4.11)$$

The heights of the maximum are $V_c=15.5kT$, $19.68kT$, $12.29kT$, $11.72kT$, and $24.3kT$ corresponding to $\omega=60$, 90, 120, 150, and 300, respectively with $kT=2.5$. Therefore, for energies around kT, the effect of the anharmonicity is small. For $\omega=120$ and 150 two other f values 40 000 and 60 000, respectively were also chosen. These f values give $62.2kT$ and $105kT$ for V_c, respectively. That the anharmonicity is small can be seen as well from the forces. Since the particle is near the bottom of a deep well, we expect that

$$\mu\omega^2x\gg\tfrac{1}{2}fx^2 \quad (4.12)$$

which is verified in the MD simulations. Another way to check this is to compute the frequency as a function of energy ϵ for a given value of f. The period, defined to be twice the time required to go from one turning point to the other is given by

$$T(\epsilon)=2\sqrt{\frac{\mu}{2}}\int_{x_-(\epsilon)}^{x_+(\epsilon)}\frac{dx}{\sqrt{\epsilon-\frac{1}{2}\mu\omega^2x^2-\frac{1}{6}fx^3}}$$

TABLE III. Dependence of frequency on energy as computed from Eq. (4.13) for a cubic oscillator with the shown (ω,f) parameters.

ϵ/kT	60, 10^4	90, 3×10^4	120, 4×10^4	120, 9×10^4	150, 6×10^4	150, 1.8×10^5	300, 10^6
1	59.45	89.35	119.73	118.60	149.80	148.16	298.26
2	58.87	88.68	119.46	117.09	149.60	146.18	296.45
3	58.25	87.97	119.18	115.47	149.40	144.03	294.58
4	57.60	87.23	118.90	113.70	149.20	141.67	292.64
5	56.90	86.45	118.62	111.75	148.99	139.06	290.63
6	56.14	85.62	118.33	109.58	148.79	136.12	288.53
7	55.32	84.75	118.03	107.11	148.58	132.75	286.33
8	54.41	83.82	117.73	104.26	148.37	128.75	284.04
9	53.41	82.83	117.44	100.08	148.16	123.79	281.63
10	52.28	81.76	117.13	96.34	147.95	117.09	279.09

$$=4\sqrt{\frac{3\mu}{f[x_+(\epsilon)-x_-(\epsilon)]}}\,K(\alpha), \tag{4.13}$$

where

$$\alpha=\frac{x_+(\epsilon)-x_-(\epsilon)}{x_+(\epsilon)-x_m(\epsilon)}, \tag{4.14}$$

with x_+, x_-, and x_m the roots of the polynomial $\epsilon-U(x)=0$ such that $x_m<x_-<x_+$ and $K(\alpha)$ is the complete elliptic integral of the first kind. Then, using $\omega(\epsilon)=2\pi/T(\epsilon)$, we display how the frequency varies with energy in Table III. We see that for energies near kT, the frequency is changed very little from its harmonic value. This is further evidence that cubic term is a small perturbation on the harmonic potential, although for $\omega=120$ and 150 at the higher f values, the frequency is perturbed considerably.

In Fig. 6, we plot the decay envelopes of the velocity autocorrelation functions computed from the molecular dynamics simulations for the five frequencies. It is interesting to note that even though the cubic anharmonicity is a small perturbation on the harmonic potential, the high frequency dephasing times are dramatically different from the harmonic results. The GLE results are also plotted in this figure. The solvent shifted values of f are obtained from the potential of mean force fit by Straub *et al.*[25] We see that even for the cubic diatomic, the GLE results are in good agreement with MD, at least in the prediction of $1/T_2$. This is a particularly interesting result, since the GLE cannot be generally derived for the case that both the bath and the bond potential are anharmonic. In the case of an anharmonic bond potential, the GLE can be derived from the harmonic bath Hamiltonian Eq. (2.44).[18,19] The agreement of the GLE with MD for the cubic potential suggests that there may be an underlying effective harmonic bath (i.e., a particular choice of the g_α's and ω_α's) which reproduces the effects of the Lennard-Jones potential at the chosen temperature and density. The GLE derived in this manner is valid even for processes far from equilibrium. For a general bath, the GLE can be derived in linear response theory, in which case, it will appear to have an effective harmonic potential. In the next section, we shall study a system in which the GLE remains valid for the anharmonic oscillator even for highly nonequilibrium states, a fact which strongly suggests the notion of an underlying effective harmonic bath.

The predictions of $1/T_2$ for given ω and f are summarized in Table IV, where we show that measured values

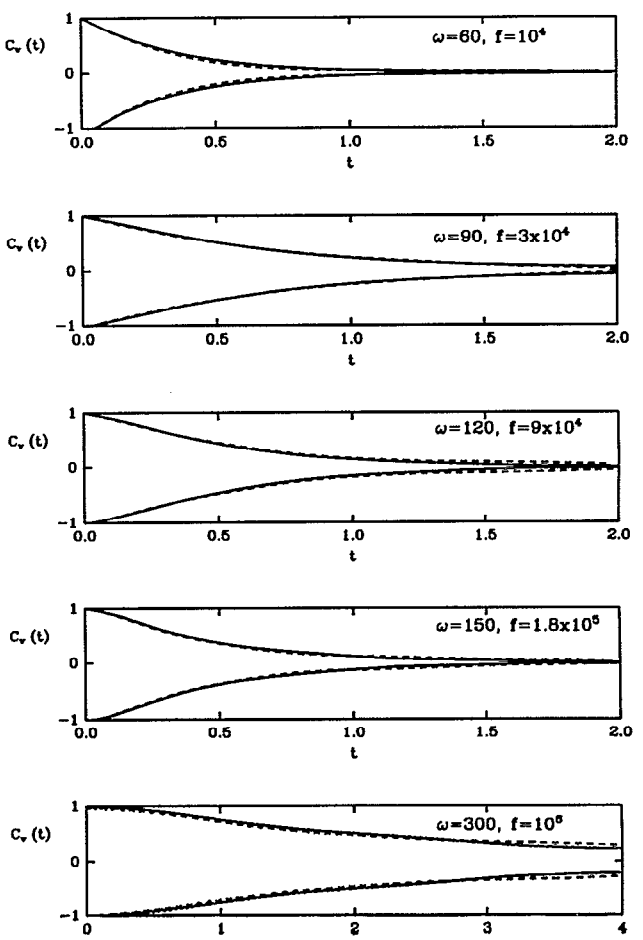

FIG. 6. Decay envelopes of the velocity autocorrelation functions from MD (solid line) and GLE (dashed line) simulations for a cubic oscillator [cf. Eq. (2.26)] in Lennard-Jones fluid for $\omega=60$, 90, 120, 150, and 300 with cubic couplings shown.

TABLE IV. Dephasing rates for cubic oscillator from MD, GLE, Eq. (2.42), Kubo theory, and modified Kubo theory.

ω	f	$\left(\frac{1}{T_2}\right)_{MD}$	$\left(\frac{1}{T_2}\right)_{GLE}$	Eq. (2.43)	Kubo	Mod. Kubo
60	10^4	3.03	3.05	3.41	0.85	3.04
90	3×10^4	1.42	1.41	1.30	0.70	1.33
120	4×10^4	0.53	0.52	0.44	0.31	0.52
120	9×10^4	1.71	1.64	0.91	0.84	1.02
150	6×10^4	0.28	0.27	0.22	0.21	0.25
150	1.8×10^5	2.00	2.01	0.85	0.79	0.86
300	10^6	0.36	0.36	0.35	0.35	0.35

from MD, GLE, Eq. (2.43), Kubo theory and a modified Kubo theory. The Kubo theory prediction is obtained by computing the fluctuating frequency and then evaluating $1/T_2^*$ from Eq. (1.4). For a derivation of the fluctuating frequency, see Appendix D. We see that the agreement is extremely poor except for the case of $\omega=300$. In light of this finding, we propose that the Kubo theory be modified to include energy relaxation according to Eq. (1.3). This modification is *ad hoc* and cannot be derived with the framework of classical Kubo theory. However, we see Table IV that including energy relaxation in the Kubo theory gives agreement with the Eq. (2.43) as expected. These results suggest that the contribution of $F_2(t)$ in $\delta\omega(t)$ [cf. Eq. (D7)] is relatively unimportant. The failure of Kubo theory at low frequency suggests that energy relaxation is an important contribution to the decay of the velocity autocorrelation function, whereas at extremely high frequency, there is almost no energy relaxation over the time needed for this function to decay so that the decay is due entirely to dephasing. The table also indicates that Eq. (2.43) fails for $\omega=120$ and 150 at the higher f values. This must be due to the fact that the cubic perturbation is too strong to be treated by perturbation theory, since for the lower values of f Eq. (2.43) predicts the relaxation rate accurately. The Kubo theory with energy relaxation is worked out to the same order in f, hence it will fail where the GLE perturbation theory fails.

C. Nonequilibrium energy decay

The GLE accurately predicts vibrational dephasing times for anharmonic diatomics in the liquid in the linear response regime. Studies of equilibrium energy relaxation for both harmonic and anharmonic diatomics show good agreement between MD and the GLE. A stringent test of the GLE, however, is its prediction of energy relaxation of anharmonic diatomics from highly nonequilibrium initial states, in which there is no *a priori* reason to believe the GLE will be valid. If an initial state is chosen not too far from equilibrium, then the energy relaxation should be well described by linear response theory

$$\frac{\bar{\epsilon}(t)-\bar{\epsilon}(\infty)}{\bar{\epsilon}(0)-\bar{\epsilon}(\infty)}=C_{\epsilon\epsilon}(t), \tag{4.15}$$

where $\bar{\epsilon}(t)$ is the average over a nonequilibrium ensemble, and $C_{\epsilon\epsilon}(t)$ is the equilibrium energy autocorrelation function. Clearly, $\bar{\epsilon}(\infty)=\langle\epsilon\rangle=kT$, which provides a criterion for knowing when the energy has relaxed. As long as the linear response theory is valid, it is expected that the GLE will agree with MD simulations of energy relaxation from the nonequilibrium state. However, it is not clear that the GLE will be able to predict energy relaxation from initial states which are not in the linear response regime. This question is examined by comparing the relaxation predicted by MD and the GLE for a diatomic with an internal Morse potential in the Lennard-Jones liquid. The Morse potential is used here instead of the cubic potential as it allows the oscillator to start at much higher energies without dissociating as would happen with the cubic potential.

The Morse potential is of the form

$$U(x)=D_0(1-e^{-\alpha x})^2, \tag{4.16}$$

where the parameters D_0 and α are chosen so that harmonic and cubic terms in the Taylor expansion of this potential match the cubic potential of Eq. (2.26), i.e.,

$$D_0=\frac{9\mu^3\omega^6}{2f^2}, \qquad \alpha=\frac{f}{3\mu\omega^2}. \tag{4.17}$$

For $\omega=120$ and $f=90\,000$, the parameters are $D_0=207.36$ and $\alpha=4.167$. Initial conditions for the oscillator are chosen such that $x(0)=0$ so that all the energy initially is kinetic. The initial velocity is chosen so as to cause the relative separation of the atoms to increase. For the MD simulations, an ensemble of initial conditions must be prepared. This is done by placing a rigid diatomic with the bond length fixed at the equilibrium separation and allowing the fluid to equilibrate around it. In order to insure that the initial conditions of the bath are distributed canonically the system is run with the newly developed Nosé–Hoover chain dynamics.[29] Once the fluid has equilibrated around the rigid diatomic, configurations are written out every 300 steps until 100 total initial states are accumulated. The 300-step time interval is long enough to avoid correlations in time between initial states. This procedure should also correspond directly to the canonical sampling of realizations of the random force which is done for the GLE simulations. Finally, to simulate the energy relaxation, the Nosé–Hoover chains are removed, and trajectories at constant total energy are run starting from each of the 100 sampled initial fluid states. The initial conditions of the diatomic are the same for all trajectories, as described above. For very high energy initial states, the giving off of energy by the diatomic to the fluid can cause the fluid to heat up, thus changing the spectral density. To minimize this effect, the fluid must contain a large number of atoms, a fact which makes the computations extremely intensive. In order to increase the efficiency of the simulations, the double RESPA scheme of Sec. III with long and short range force breakup is used [cf. Eqs. (3.10) and (3.11)]. This gives an overall factor of 32 in the time step over velocity Verlet, and an overall saving in CPU time of 16 over velocity Verlet.

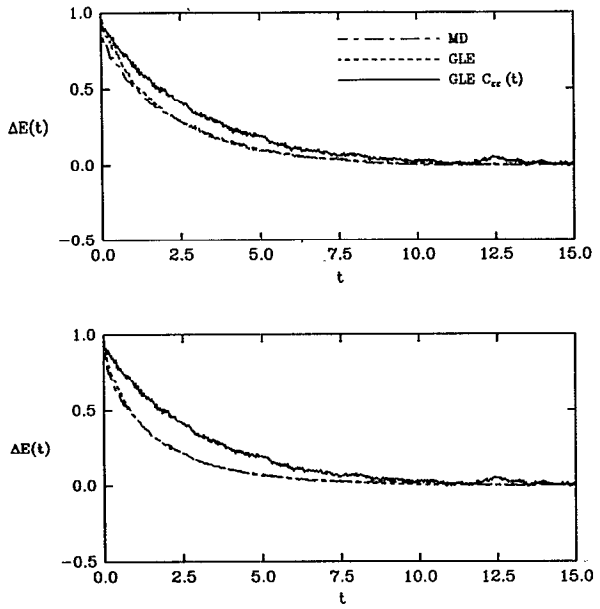

FIG. 7. Nonequilibrium energy decay from the left side of Eq. (4.15) for a Morse oscillator in a Lennard-Jones fluid as computed from the GLE (dashed line) and MD (double dashed line) using 500 particles for initial conditions corresponding to energies of $20kT$ (upper curve) and $40kT$ (lower curve). Also shown in each figure, with a solid line, is the equilibrium energy autocorrelation function (i.e., linear response theory) from full GLE simulations.

MD simulations using 500 fluid atoms and a single diatomic were run for initial oscillator energies of $20kT$, and $40kT$ as well as GLE simulations. GLE simulations were also run for a variety of low energies to determine how high the energy of the diatomic must be in order to be outside the linear response regime. It was found that the linear response theory Eq. (4.15) is valid up to energies around $10kT$ for this system so that energies of 20 and $40kT$ are well outside this regime. In Fig. 7, we show the comparison of the MD and GLE simulations of the nonequilibrium energy decay [i.e., the left side of Eq. (4.15)]. Also shown in the figure is the equilibrium energy autocorrelation function for the Morse potential determined from the full GLE simulations of Sec. IV B. We see that even up to energies of $20kT$ and $40kT$, the GLE predicts very accurately, the nonequilibrium relaxation rate, even though these are not well described by linear response theory. In addition, MD and GLE simulations were also run for a harmonic diatomic far from equilibrium for initial bond energies up to $90kT$, and all were found to be well described by linear response theory.

In all cases studied, the nonlinear GLE predicts that the energy relaxes faster than or is bounded from above by what would be predicted by the GLE in the linear response regime. This is expected since, for the nonlinear oscillator, the vibrational period is an increasing function of the vibrational energy. (The vibrational frequency is therefore a decreasing function of energy—cf. Table III.) Hence, a highly excited oscillator will have a vibrational frequency lying closer to the accepting modes of the bath and will thus exchange energy with the bath more readily. As the oscillator relaxes, its vibrational frequency gets larger and detunes away from the bath modes with the result that the vibrational energy transfer slows down and eventually overlaps what is observed in the linear response regime. This is similar to what was observed in the relaxation of I_2 and Br_2 in argon.[30,31]

To understand these results, consider that when the bond potential and the bath are both anharmonic, then the GLE cannot be shown to be a valid description of the system. However, if the bath can be well described by an equivalent effective harmonic bath, then the GLE should be valid for any bond potential even far from equilibrium. These results suggest, then, that there should be an effective harmonic bath underlying the true Lennard-Jones fluid used for these studies. The notion of an underlying effective harmonic bath for this system is not altogether surprising when one considers that the reduced density $\rho\sigma^3 = 1.05$ is just below the crystal density for reduced temperature $\hat{T} = 2.5$ Although the fluid is a hot, dense fluid, it is not far from the solid phase. It is expected that if the density were lowered, the notion of an underlying effective harmonic bath would break down as strong impulsive collisions would become increasingly important. In this case, the GLE with a Gaussian random force would probably not be a good description of the nonequilibrium energy decay. However, as discussed in Sec. IV A, if impulsive, Poissonian type collisions could be built into it, the GLE might serve as a good description for the general bath.

V. CONCLUSION

In this paper full molecular dynamics simulations of vibrational relaxation in simple fluids show that the generalized Langevin equation is an excellent quantitative model. We have derived expressions for the velocity, position, and energy autocorrelation functions from the GLE for a harmonic potential of mean force and extracted the relaxation time T_2 and T_1 from these. We have also used perturbation theory to derive the vibrational relaxation time T_2 from the GLE with cubic anharmonicity. These results have been compared to full molecular dynamics simulations of a single oscillator at high frequency and a range of cubic couplings in a Lennard-Jones fluid. In order to solve the multiple time scale problem, the reversible version of RESPA presented in Sec. III and a new multiple time scale algorithm for the GLE based on the reversible version of RESPA were used. The friction kernel for the GLE was calculated using the method of Straub and Berne[5] or that of Ref. 7 from the force autocorrelation function on a rigid diatomic. The GLE and MD were found to be in good agreement for both predictions of T_1 and T_2 for the harmonic diatomic. At high frequency, a small discrepancy was found between the GLE and MD for T_1. We attribute this to the fact that the GLE misses the rare impulsive collisions which occur in real systems by assuming the random force is a Gaussian random process. Therefore, this discrepancy is expected to grow as the fre-

quency increases, and could become important at low frequencies for less dense systems. We derived an expression for the deviation in the energy autocorrelation function in the Gaussian random force approximation and the true energy autocorrelation function for short times and found the predicted discrepancy consistent with our observations from the GLE-MD comparison.

The predictions of vibrational relaxation times of an anharmonic diatomic with cubic anharmonicity from MD and the GLE were also compared. These were found to be in good agreement at all frequencies and cubic couplings. The perturbation theory result Eq. (2.43) was found to break down for $\omega=120$ and 150, when f was too large. When the perturbation was made smaller, the agreement was better. The MD and GLE results were also compared to Kubo theory, which was found to be in poor agreement with the simulation results for all except the highest frequency ($\omega=300$). We conjecture that the breakdown of Kubo theory is due to the fact that energy relaxation can contribute significantly to the vibrational relaxation of an anharmonic oscillator at low frequencies, and Kubo theory leaves this contribution out. By modifying Kubo theory to include the energy relaxation, the modified predictions were found to be in much better agreement with the simulation results. Since the GLE cannot be shown to be valid for an anharmonic diatomic interacting with an anharmonic bath, except in linear response, the agreement of the GLE with MD for all frequencies and cubic couplings is somewhat surprising. The GLE can be derived from the harmonic bath Hamiltonian, however, a fact which suggests that the Lennard-Jones bath at $\hat{T}=2.5$ and $\rho\sigma^3=1.05$ may be well described by an underlying effective harmonic bath.

To test the validity of the GLE for nonlinear oscillators and the notion that the bath may be well described well by an underlying effective harmonic bath, the energy relaxation from nonequilibrium states for a diatomic with an internal Morse potential was studied. The parameters of the Morse potential were chosen to agree with the cubic potential for $\omega=120$ and $f=90\,000$ by expanding the Morse potential and equating the harmonic and cubic terms. It was found that, even when the nonequilibrium decay was poorly described by linear response theory, the simulation of the nonlinear GLE predicted the same relaxation rate as MD. Whitnell *et al.*[32] have numerically simulated the vibrational energy relaxation of aqueous CH_3Cl treated like a diatomic for several different sets of charges on CH_3Cl and report that even for high excitation energies, linear response theory and the Landau–Teller theory [cf. Eq. (1) of Ref. 32] accurately predicts the simulation results. Their system differs from ours in several important respects. Because the molecular vibration is not far off resonance with the water librational modes, the relaxation is very fast and dominated by long range interactions. When the charges are turned off, the decay is too slow for analysis. By contrast, our system is short ranged and off resonance. Hence, a different physical response is not surprising. RESPA allows study of such previously inaccessible decays as are encountered, for example, in the diatomic potentials studied here. As expected, the nonequilibrium relaxation of a harmonic diatomic, a linear system, was found to agree with linear response theory for all initial states up to $90kT$. The fact that the GLE predicts the same relaxation rate as MD even for highly nonequilibrium states supports the notion that the fluid can be well described by an effective bath. It is expected that for lower densities, in which impulsive collisions will be more frequent and more important, the GLE would begin to break down for highly nonequilibrium initial states. However, if the GLE could be supplemented to include the impulsive Poissonian type collisions along with the Gaussian random force in a way which preserved the second fluctuations dissipation theorem, then the range of validity would, most likely, be increased to include low density, high temperature situations.

ACKNOWLEDGMENTS

We wish to thank Professor Eli Pollak and Dr. Joel Bader for many useful discussions. This project was funded by a grant from the National Science Foundation. In addition, the numerical simulations were done on the computational facilities at the Thomas J. Watson Research Laboratories of IBM and on the CRAY Y-MP at NCSA, University of Illinois.

APPENDIX A: DERIVATION OF EQ. (2.7)

In this Appendix we show how Eq. (2.7) can be derived starting from the formal solutions Eq. (2.10) of the GLE. The energy of the oscillator is $\epsilon=\mu v^2/2+\mu\omega^2x^2/2$ so that, using these solutions, the quantity $\langle\epsilon(0)\epsilon(t)\rangle$ can be expressed as

$$\langle\epsilon(0)\epsilon(t)\rangle=\frac{\mu^2}{4}\langle v^4\rangle[C_{vv}^2(t)+\omega^2C_{vx}^2(t)]+\frac{\mu^2\omega^2}{4}\langle x^4\rangle[\omega^2C_{xx}^2(t)+C_{xv}^2(t)]+\frac{\mu^2}{4}\langle x^2v^2\rangle[C_{xv}^2(t)+\omega^4C_{vx}^2(t)+\omega^2C_{vv}^2(t)$$

$$+\omega^2C_{xx}^2(t)]+\frac{\mu^2}{4}(\langle v^2\rangle+\omega^2\langle x^2\rangle)\int_0^t d\tau_1\int_0^t d\tau_2[C_{vv}(\tau_1)C_{vv}(\tau_2)+\omega^2C_{vx}(\tau_1)C_{vx}(\tau_2)]$$

$$\times\langle R(t-\tau_1)R(t-\tau_2)\rangle. \tag{A1}$$

From the second fluctuation dissipation theorem, we have

$$\langle R(t-\tau_1)R(t-\tau_2)\rangle=\frac{kT}{\mu}\gamma(\tau_2-\tau_1)\theta(\tau_2-\tau_1), \tag{A2}$$

where $\theta(t)$ is the Heavyside step function. Using Eq. (A2), the relation $C_{xv}(t)=-\omega^2 C_{vx}(t)$, and the expressions in Sec II A for the equilibrium moments, Eq. (A1) becomes

$$\langle\epsilon(0)\epsilon(t)\rangle=(kT)^2\left[C_{vv}^2(t)+C_{xx}^2(t)+\frac{2}{\omega^2}C_{xv}^2(t)\right]+\frac{(kT)^2}{2}\int_0^t d\tau_2\int_0^{\tau_2}d\tau_1\,\gamma(\tau_2-\tau_1)\times[C_{vv}(\tau_1)C_{vv}(\tau_2)+\omega^2 C_{vx}(\tau_1)C_{vx}(\tau_2)]. \tag{A3}$$

Using the identities Eqs.(2.11) and (2.12), it follows that

$$\begin{aligned}&\int_0^t d\tau_2\,C_{vv}(\tau_2)\int_0^{\tau_2}d\tau_1\,C_{vv}(\tau_1)\gamma(\tau_2-\tau_1)\\&=\int_0^t d\tau_2\,C_{vv}(\tau_2)\left[-\frac{d}{d\tau_2}C_{vv}(\tau_2)-\omega^2\int_0^{\tau_2}d\tau_1\,C_{vv}(\tau_1)\right]\\&=-\frac{1}{2}\int_0^t d\tau_2\frac{d}{d\tau_2}C_{vv}^2(\tau_2)-\omega^2\int_0^t d\tau_2\,C_{vv}(\tau_2)C_{vx}(\tau_2)\\&=-\frac{1}{2}[C_{vv}^2(t)-1]-\omega^2\int_0^t d\tau\,C_{vv}(\tau)C_{vx}(\tau)\end{aligned} \tag{A4}$$

and similarly that

$$\begin{aligned}&\omega^2\int_0^t d\tau_2\,C_{vx}(\tau_2)\int_0^{\tau_2}d\tau_1\,C_{vx}(\tau_1)\gamma(\tau_2-\tau_1)\\&=-\frac{1}{2\omega^2}C_{xv}^2(t)+\omega^2\int_0^t d\tau\,C_{vx}(\tau)C_{xx}(\tau).\end{aligned} \tag{A5}$$

Furthermore, we see that

$$\begin{aligned}\int_0^t d\tau\,C_{vx}(\tau)C_{xx}(\tau)&=-\frac{1}{\omega^2}\int_0^t d\tau\,C_{xx}(\tau)\frac{d}{d\tau}C_{xx}(\tau)\\&=-\frac{1}{2\omega^2}[C_{xx}^2(t)-1]\end{aligned} \tag{A6}$$

and

$$\begin{aligned}\int_0^t d\tau\,C_{vx}(\tau)C_{vv}(\tau)&=\int_0^t d\tau\,C_{vx}(\tau)\frac{d}{d\tau}C_{vx}(\tau)\\&=\frac{1}{2}C_{vx}^2(t).\end{aligned} \tag{A7}$$

When Eqs.(A6) and (A7) are substituted into Eqs.(A4) and (A5) and the results are then substituted into Eq. (A3), we find, after subtracting off the equilibrium value and normalizing, that we recover Eq. (2.7)

$$C_{\epsilon\epsilon}(t)=\frac{1}{2}C_{vv}^2(t)+\frac{1}{2}C_{xx}^2(t)+\frac{1}{\omega^2}[\dot{C}_{xx}(t)]^2. \tag{A8}$$

APPENDIX B: ANALYTICAL SOLUTION OF THE CUBIC OSCILLATOR REFERENCE SYSTEM

In Sec. III, we discussed the use of an analytical reference system for the harmonic diatomic and mentioned that an analytical solution for the cubic oscillator can be expressed in terms of Jacobi elliptic functions. The reference system equation of motion will be of the form

$$\ddot{x}=\frac{1}{\mu}F_r(x)=-\omega^2 x-\frac{f}{2\mu}x^2. \tag{B1}$$

The time evolution of the initial state $\{x(0),\dot{x}(0)\}$ for a time step Δt under the action of the reference system propagator $\exp(iL_r\Delta t)$ is then given by

$$e^{iL_r\Delta t}x(0)=x_+-(x_+-x_-)\times sn^2\left(\sqrt{\frac{1}{2}\frac{f(x_+-x_m)}{3\mu}}\,(\Delta t+v)\,|\,\alpha\right), \tag{B2}$$

where $sn(x)$ is the Jacobi elliptic function, v is the incomplete elliptic integral

$$v=2\sqrt{\frac{3\mu}{f(x_+-x_m)}}\int_0^{\phi}\frac{d\theta}{\sqrt{1-\alpha\sin^2\theta}}. \tag{B3}$$

Also

$$\sin\phi=\sqrt{\frac{x_+-x(0)}{x_+-x_-}} \tag{B4}$$

and

$$\alpha=\frac{x_+-x_-}{x_+-x_m}. \tag{B5}$$

The quantities x_m, x_+, and x_- are the roots of the polynomial $(x_m<x_-<x_+)$

$$E-\tfrac{1}{2}\mu\omega^2x^2-\tfrac{1}{6}fx^3=0 \tag{B6}$$

with the energy E determined from the initial conditions. The velocity can either be obtained by direct differentiation of by use of the formula

$$\mu\dot{x}=\sqrt{2\mu(E-\tfrac{1}{2}\mu\omega^2x^2-\tfrac{1}{6}fx^3)}\,. \tag{B7}$$

Since the solutions are complicated functions of the initial conditions, the Jacobi elliptic function and incomplete elliptic integral must be evaluated at every time step. However, given fast codes for these functions, such as are found in *Numerical Recipes*,[33] using the analytical solution can still be a significant savings over a numerical one.

APPENDIX C: DERIVATION OF EQ.(4.9)

The derivation of Eq. (4.9) requires that we compute the difference between the true energy autocorrelation function and the Gaussian approximation Eq. (2.7) to $\mathcal{O}(t^4)$. To obtain the expansion Eq. (2.7), we note that the velocity autocorrelation function has an expansion of the form

$$C_{vv}(t)=1+\frac{1}{2}\frac{d^2C_{vv}}{dt^2}(0)t^2+\frac{1}{24}\frac{d^4C_{vv}}{dt^4}(0)t^4+\cdots \tag{C1}$$

and similarly for $C_{xx}(t)$ because the odd derivatives vanish at $t=0$. Since $C_{vv}(t)\sim\langle v(0)\exp(iLt)v(0)\rangle$, it is easily seen that $d^2C_{vv}(0)/dt^2\sim\langle\dot{v}^2\rangle$ and $d^4C_{vv}(0)/dt^4\sim\langle\ddot{v}^2\rangle$, etc. Substituting the expansions of $C_{vv}(t)$, $C_{xx}(t)$, and $\dot{C}_{xx}(t)$ into Eq. (2.7), and using the facts that $\langle v^2\rangle=\omega^2\langle x^2\rangle$ and $\langle a^2\rangle=-\langle a'\rangle/\beta\mu$, where a is the acceleration and a' is the derivative of the acceleration with respect to position gives the expansion of the Gaussian approximation to the energy autocorrelation function

$$C_{\epsilon\epsilon}^{(G)}(t)=1+\frac{1}{2}[\langle a'\rangle+\omega^2]t^2+\left[\frac{1}{24}\langle a'^2\rangle+\frac{1}{8}\langle a'\rangle^2+\frac{7}{24}\omega^2\langle a'\rangle+\frac{\omega^2}{8}\right]t^4. \tag{C2}$$

The expansion of the true energy autocorrelation function takes the same form as Eq. (C1) with the coefficients of t^2 and t^4 being given by the averages $\langle\dot{\epsilon}\rangle$ and $\langle\ddot{\epsilon}\rangle$, respectively. With $\epsilon=\mu v^2/2+\mu\omega^2x^2/2$, it is clear that there will be a large number of terms. All these terms can be simplified using a general identity

$$\langle f(x,a)a\rangle=-\frac{1}{\beta\mu}\left\langle\frac{d}{dx}f(x,a)\right\rangle=-\frac{1}{\beta\mu}\left\langle\left(\frac{\partial f}{\partial x}+\frac{\partial f}{\partial a}a'\right)\right\rangle, \tag{C3}$$

which can be derived by noting that

$$\langle f(x,a)a\rangle\sim\int dx\,f(x,a)\frac{1}{\beta\mu}\frac{\partial}{\partial x}e^{-\beta U(x)} \tag{C4}$$

and integrating by parts. Using the identity Eq. (C3), the expansion of the true energy autocorrelation function can be shown to be

$$C_{\epsilon\epsilon}(t)=1+\frac{1}{2}[\langle a'\rangle+\omega^2]t^2+\left[\frac{1}{6}\langle a'^2\rangle+\frac{1}{8}\omega^4+\frac{1}{24}\langle aa'\rangle-\frac{\beta\mu\omega^4}{24}\langle x^2a'\rangle+\frac{\omega^2}{3}\langle a'\rangle+\frac{\omega^2}{12}\langle xa''\rangle\right]t^4. \tag{C5}$$

Computing the difference $\Delta_\epsilon^{(4)}(t)=C_{\epsilon\epsilon}(t)-C_{\epsilon\epsilon}^{(G)}(t)$ and using the identity Eq. (C3) a few more times, it is straightforward to derive Eq. (4.9).

APPENDIX D: CLASSICAL DERIVATION OF THE FLUCTUATING FREQUENCY

In this Appendix, we give a classical derivation of the fluctuating frequency used to calculate $1/T_2$ in the Kubo theory. If $V(x,\{r\})$ represents the coupling potential between the relative coordinate x of the diatomic and the bath coordinates $\{r\}$, then following Oxtoby,[12,13] we may expand the potential in a power series in x

$$V(x,\{r\})=V_0+F_1(t)x+F_2(t)x^2+\cdots, \tag{D1}$$

where the time-dependent coefficients depend on the motion of the bath degrees of freedom [i.e., $F_1(t)\equiv F_1(\{r\};t)$, etc.]. Furthermore, if the bond potential is taken to have both harmonic and cubic terms, then the total potential involving x is

$$U+V=V_0+F_1(t)x+F_2(t)x^2+\tfrac{1}{2}\mu\omega^2x^2+\tfrac{1}{6}fx^3. \tag{D2}$$

We are interested in the high frequency limit in which the coupling to the bath is weak and may be considered a small perturbation to the bond potential. By completing the square, we may write the total potential as

$$U+V=V_0(t)+\frac{1}{2}\mu\omega^2\left[x+\frac{F_1(t)}{\mu\omega^2}\right]+F_2(t)x^2+\frac{1}{6}fx^3, \tag{D3}$$

where $V_0(t)=V_0-F_1^2(t)/2\mu\omega^2$. We now introduce a change of variables

$$y=x+\frac{F_1(t)}{\mu\omega^2} \tag{D4}$$

in terms of which the potential becomes

$$U+V=V_0(t)+\frac{1}{2}\mu\omega^2y^2+F_2(t)\left[y-\frac{F_1(t)}{\mu\omega^2}\right]^2+\frac{1}{6}f\left[y-\frac{F_1(t)}{\mu\omega^2}\right]^3. \tag{D5}$$

By working to first order in F_1 and F_2, we find the potential becomes

$$U+V=V_0(t)+\frac{1}{2}\mu\left[\omega^2+\frac{2F_2}{\mu}-\frac{fF_1(t)}{\mu^2\omega^2}\right]y^2+\frac{1}{6}fy^3 \tag{D6}$$

from which we see that the fluctuating frequency is given by

$$\omega(t)=\sqrt{\omega^2+\frac{2F_2(t)}{\mu}-\frac{fF_1(t)}{\mu^2\omega^2}}\approx\omega+\frac{F_2(t)}{\mu\omega}-\frac{fF_1(t)}{2\mu^2\omega^3}. \tag{D7}$$

Oxtoby obtained the same result using quantum mechanical perturbation theory.

Expressions for $F_1(t)$ and $F_2(t)$ can be easily computed from the potential. The terms in the potential energy involving the coordinates of the diatomic take the form

$$U=\sum_j[V(\mathbf{x}_1)+V(\mathbf{x}_2)], \tag{D8}$$

where V is the site–site potential, and

$$\mathbf{x}_1=\mathbf{R}+\tfrac{1}{2}r\mathbf{u}-\mathbf{r}_j,\qquad\mathbf{x}_2=\mathbf{R}-\tfrac{1}{2}r\mathbf{u}-\mathbf{r}_j \tag{D9}$$

with $\mathbf{R}$ the center of mass, r the relative coordinate, $\mathbf{u}$ the unit vector along the bond, and $\mathbf{r}_j$ the position of the j the solvent atom. The necessary derivatives are

$$\frac{\partial U}{\partial r}=\frac{1}{2}\left[\frac{\partial V}{\partial\mathbf{x}_1}-\frac{\partial V}{\partial\mathbf{x}_2}\right]\cdot\mathbf{u},\qquad\frac{\partial^2U}{\partial r^2}=\frac{1}{4}\left[\frac{\partial^2V}{\partial\mathbf{x}_1\mathbf{x}_1}+\frac{\partial^2V}{\partial\mathbf{x}_2\mathbf{x}_2}\right]\cdot\cdot\,\mathbf{uu}. \tag{D10}$$

The dyads in the above expression are simply

$$\frac{\partial V}{\partial \mathbf{x}_i}=\frac{dV}{d\rho}\frac{\mathbf{x}_i}{\rho},$$
$$\frac{\partial^2 V}{\partial \mathbf{x}_i \mathbf{x}_i}=\frac{d^2V}{d\rho^2}\frac{\mathbf{x}_i\mathbf{x}_i}{\rho^2}+\frac{1}{\rho}\frac{dV}{d\rho}\left(\mathbf{I}-\frac{\mathbf{x}_i\mathbf{x}_i}{\rho^2}\right), \tag{D11}$$

where $\rho \equiv |\mathbf{x}_i|$, and $V(\rho)$ is just the functional form of the site–site potential.

Note that the coupling to the bath is a second order effect in the fluctuating frequency in the sense that if $f=0$, $\omega(t)$ only involves $F_2(t)$. The presence of an anharmonicity is required to bring in the first order coupling to the bath. It is evident, furthermore, that in a perturbation theory scheme, a lowest order linear system based on $\omega(t)$ will be a better approximation to the linear system than one based simply on ω since $\omega(t)$ takes into account some effect of the anharmonicity.

By defining $\delta\omega(t)\equiv\omega(t)-\bar{\omega}$, we have an expression for the fluctuations in the frequency which can be easily computed in a molecular dynamics calculation and autocorrelated to give the dephasing contribution to $1/T_2$ according to Eq. (1.4).

[1] S. Klippenstein and J. T. Hynes, J. Phys. Chem. **95**, 4651 (1991).
[2] A. M. Levine, M. Shapiro, and E. Pollak, J. Chem. Phys. **88**, 1959 (1988).
[3] B. J. Berne, M. Borkovec, and J. E. Straub, J. Phys. Chem. **92**, 3711 (1988).
[4] H. Mori, Prog. Theor. Phys. **33**, 423 (1965).
[5] J. E. Straub, M. Borkovec, and B. J. Berne, J. Phys. Chem. **91**, 4995 (1987).
[6] J. Straub, B. J. Berne, and B. Roux, J. Chem. Phys. **93**, 6804 (1990).
[7] B. J. Berne, M. E. Tuckerman, J. E. Straub, and A. L. R. Bug, J. Chem. Phys. **93**, 5084 (1990).
[8] Z. Schuss, *Theory and Applications of Stochastic Differential Equations* (Wiley, New York, 1980).
[9] L. M. Delves and J. L. Mohamed, *Computational Methods for Integral Equations* (Cambridge University, New York, 1985).
[10] R. Kubo, Adv. Chem. Phys. **13**, 101 (1963); J. Math. Phys. **4**, 174 (1963).
[11] R. Kubo, *Fluctuations, Relaxation, and Resonance in Magnetic Systems*, edited by D. Ter Haar (Plenum, New York, 1962).
[12] D. Oxtoby, J. Chem. Phys. **70**, 2605 (1979).
[13] D. Oxtoby, D. Levesque, and J. Weiss, J. Chem. Phys. **68**, 5528 (1978).
[14] M. Tuckerman, G. Martyna, and B. J. Berne, J. Chem. Phys. **93**, 1287 (1990).
[15] M. E. Tuckerman and B. J. Berne, J. Chem. Phys. **95**, 8362 (1991).
[16] M. E. Tuckerman, G. J. Martyna, and B. J. Berne, J. Chem. Phys. **97**, 1990 (1992).
[17] G. Arfken, *Mathematical Methods for Physicists* (Academic, Orlando 1985).
[18] R. Zwanzig, J. Stat. Phys. **9**, 215 (1973).
[19] A. O. Caldeira and A. J. Leggett, Ann. Phys. **149**, 374 (1983).
[20] Y. I. Georgievskii and A. A. Stuchebrukhov, J. Chem. Phys. **93**, 6699 (1990).
[21] M. E. Tuckerman and B. J. Berne, J. Chem. Phys. **95**, 4389 (1991).
[22] S. O. Rice, Bell Tel. J. **23**, 282 (1944).
[23] S. O. Rice, Bell Tel J. **25**, 46 (1945).
[24] M. C. Wang and G. E. Uhlenbeck, Rev. Mod. Phys. **17**, 323 (1945).
[25] J. E. Straub, M. Borkovec, and B. J. Berne, J. Chem. Phys. **89**, 4833 (1988).
[26] S. A. Rice and A.R. Allnatt, J. Chem. Phys. **34**, 2144 (1961).
[27] A. R. Allnatt and S. A. Rice, J. Chem. Phys. **34**, 2156 (1961).
[28] B. J. Berne, J. L. Skinner, and P. G. Wolynes, J. Chem. Phys. **73**, 4314 (1980).
[29] G. J. Martyna, M. Klein, and M Tuckerman, J. Chem. Phys. **97**, 2635 (1992).
[30] J. T. Hynes, R. Kapral, and G. M. Torrie, J. Chem. Phys. **72**, 177 (1980).
[31] F. G. Amar and B. J. Berne, J. Phys. Chem. **88**, 6720 (1984).
[32] R. M. Whitnell, K. R. Wilson, and J. T. Hynes, J. Phys. Chem. **94**, 8628 (1991).
[33] W. H. Press, B. P. Flannery, S. A. Teukolsky, and W. T. Vetterling, *Numerical Recipes* (Cambridge University, Cambridge, 1986).